The LINNEAN SOCIETY of London ZOOLOGICAL Journal of the Linnean Society

Zoological Journal of the Linnean Society, 2012, **166**, 876–911. With 22 figures

Comparative osteology and phylogenetic relationships of *Miocaperea pulchra*, the first fossil pygmy right whale genus and species (Cetacea, Mysticeti, Neobalaenidae)

MICHELANGELO BISCONTI*

Museo di Storia Naturale del Mediterraneo, Via Roma 234, 57125, Livorno, Italy

Received 18 August 2011; revised 6 July 2012; accepted for publication 26 July 2012

A fossil pygmy right whale (Cetacea, Mysticeti, Neobalaenidae) with exquisitely preserved baleen is described for the first time in the history of cetacean palaeontology, providing a wealth of information about the evolutionary history and palaeobiogeography of Neobalaenidae. This exquisitely preserved specimen is assigned to a new genus and species, ***Miocaperea pulchra* gen. et sp. nov.**, and differs from *Caperea marginata* Gray, 1846, the only living taxon currently assigned to Neobalaenidae, in details of the temporal fossa and basicranium. A thorough comparative analysis of the skeleton of ***M. pulchra* gen. et sp. nov.** and *C. marginata* is also provided, and forms the basis of an extensive osteology-based phylogenetic analysis, confirming the placement of ***M. pulchra* gen. et sp. nov.** within Neobalaenidae as well as the monophyly of Neobalaenidae and Balaenidae; the phylogenetic results support the validity of the superfamily Balaenoidea. No relationship with Balaenopteroidea was found by the present study, and thus the balaenopterid-like morphological features observed in *C. marginata* must have resulted from parallel evolution. The presence of ***M. pulchra* gen. et sp. nov.** around 2000 km north from the northernmost sightings of *C. marginata* suggests that different ecological conditions were able to support pygmy right whale populations in what is now Peru, and that subsequent environmental change caused a southern shift in the distribution of the living neobalaenid whales.

doi: 10.1111/j.1096-3642.2012.00862.x

ADDITIONAL KEYWORDS: Balaenoidea – *Caperea marginata* – Miocene – Peru – phylogeny.

INTRODUCTION

In the last few decades the evolutionary history of baleen whales (Mammalia, Cetacea, Mysticeti) has been investigated by morphological and molecular analyses, but only a limited consensus has emerged from this effort. One of the major points of disagreement concerns the phylogenetic relationships of the pygmy right whale *Caperea marginata* Gray, 1846, the only species currently assigned to the family Neobalaenidae (Baker, 1985). In fact, most morphological analyses support a close relationship of Neobalaenidae and Balaenidae (right and bowhead whales; Bisconti, 2005; Deméré, Berta & McGowen, 2005), but the molecular and few morphological studies performed have almost invariably indicated a close relationship of Neobalaenidae and the Eschrichtiidae–Balaenopteridae clade (gray, rorqual, and humpback whales; Sasaki *et al*., 2005; Nikaido *et al*., 2006; Deméré *et al*., 2008).

Neobalaenids are characterized by balaenid-like features, such as: arched rostrum; high number of long baleen plates; fused cervical vertebrae; low and

*E-mail: zoologia.museo@provincia.livorno.it

wide tympanic bulla, with low tympanic cavity; anteriorly thrusted supraoccipital that is superimposed on the parietal, preventing the parietal from appearing at the skull vertex; and alimentary behaviour based on continuous ram feeding to exploit calanoid copepods (Beddard, 1901; Baker, 1985). Balaenopterid- and eschrichtiid-like features include: presence of ventral throat grooves in some individuals; squamosal cleft; a dorsal fin, radius, and ulna longer than humerus; and flat supraorbital process of the frontal (Baker, 1985; Marx, 2010). Given that *C. marginata* possesses a mix of balaenid and balaenopterid characters, it is difficult to understand which features are the result of convergence and which are those representing the proof of true phylogenetic relationships. Up to present times, the fossil record could not help reconstruct the ancestral morphological conditions of Neobalaenidae because it was considered to be non-existent (Fordyce & De Muizon, 2001; Fordyce, 2009). A recent find from New Zealand suggested that neobalaenid whales were existent in the southern hemisphere around 6.2–5.4 Mya (Fitzgerald, 2012), but the find consisted of a single posterior process of a periotic that is not diagnostic enough to provide information about taxonomy and phylogenetic relationships.

In this article, the anatomy of an exquisitely preserved neobalaenid skull is reported and its phylogenetic implications are discussed. The new specimen is the holotype of *Miocaperea pulchra* gen. et sp. nov., found from the upper Miocene Pisco Formation at Aguada de Loma, Peru (Fig. 1), and is now permanently housed in the Staatliches Museum für Naturkunde, Stuttgart, Germany, as specimen no. 46978 of the palaeontological collection. The specimen was excavated by Jakob Siber in 1985, and was legally exported by the Siber+Siber Aathal/Zürich company (E.P.J. Heizmann, pers. comm.). Mr Siber confirmed the legal status of the specimen before the Society of Friends of the Natural History Museum Stuttgart bought it (E.P.J. Heizmann, pers. comm.). The legal documentation can be provided by Siber+Siber Aathal/Zürich. The specimen came to the Stuttgart collection as a present from the Society of Friends of the State Museum of Natural History (SMNS), together with further Peruvian material (e.g. the skeleton of *Balaenoptera siberi* Pilleri, 1989, which is exhibited in the Schloss Rosenstein building of the SMNS).

Detailed comparisons with the living pygmy right whale *C. marginata* are provided to form a solid basis for a new and comprehensive cladistic analysis of Mysticeti, directed at discovering the phylogenetic relationships of Neobalaenidae. An in-depth analysis of the basicranium, earbones, and postcranial skeleton of the extant *C. marginata* are included to supplement the section dealing with the compara-

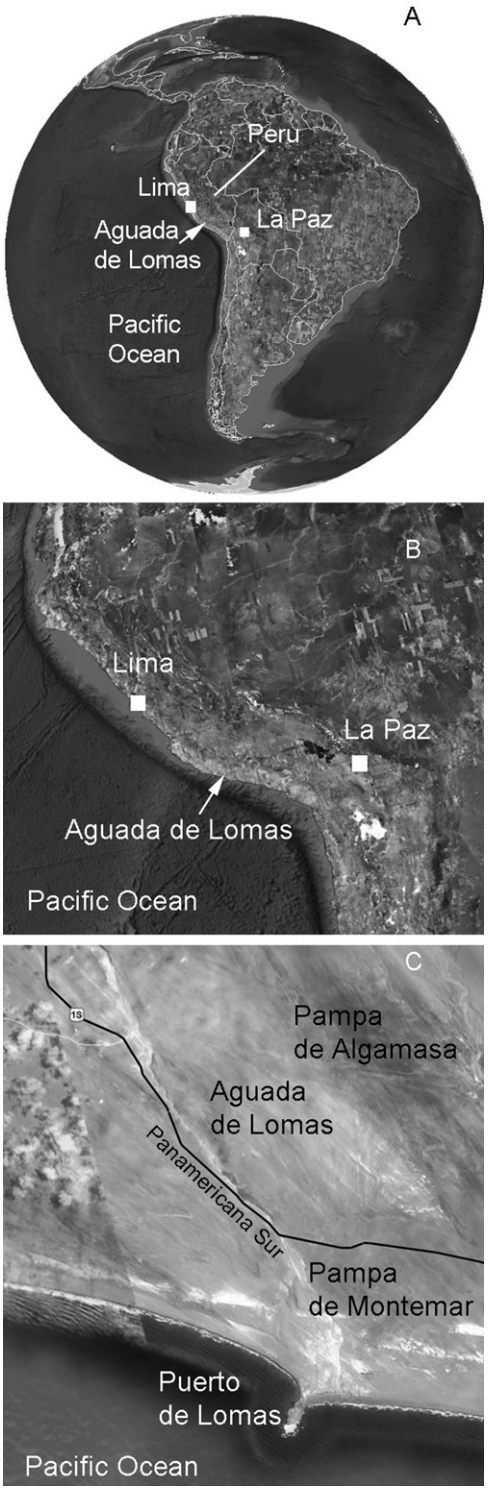

Figure 1. Locality of the discovery of ***Miocaperea pulchra* gen. et sp. nov.** A, South America; B, Peruvian territory with Aguada de Lomas indicated by a line; C, close-up view of Aguada de Lomas in Peru.

tive anatomy of *M. pulchra* gen. et sp. nov., so as to provide the first detailed morphological descriptions of some anatomical parts of the neobalaenid skeleton, and to provide data about individual variation and the growth trajectory of *C. marginata*.

In this article, the anatomical terminology is taken from Mead and Fordyce (2010) and, for limited parts, from Nickel *et al*. (1999), Schaller (1999), and Struthers (1895).

Anatomical abbreviations: aar, area of acetabulum in the pelvis; ab-pch, anterior border of pars cochlearis; ae, anterior end of pelvis; afa, atlas articular facet for occipital condyle; afi, (incus) articular facet for malleus; alc, anterolateral corner; amc, anteromedial corner; ang, angular process of dentary; ap, acromion process of scapula; aplf, area of posterior ligament of femur in the pelvis; app, anterior process of periotic; b, baleen; bC5 and bC6, body of cervical vertebrae 5 and 6; bdp, basioccipital descending process; bg, groove for vasculature of the baleen-bearing epithelium; boc, basioccipital; bst, base of stapes; c, coana; C2–C7, cervical vertebrae 2–7; cb, crus breve (incus); cdp, caudal process of periotic; cop, conical process; cp, coracoid process of scapula; cs, cranial surface of periotic; cu, cuneiform; dc, dorsal crest of periotic; eam external acoustic meatus; da, dorsal apophysis; daa, dorsal apophysis of atlas; der, distal epiphysis of radius; deu, distal epiphysis of ulna; dpt, deltopectoral tuberosity of humerus; dr, diaphysis of radius; du, diaphysis of ulna; efc, external opening of facial canal; elf, endolymphatic duct; eof, external opening of the facial canal; etr, epitympanic recess; exo, exoccipital; fi, fossa incudis; f-iop, fissure in infraorbital plate of maxilla; flp, foramen lacerus posterius; fm, foramen magnum; fpo, foramen pseudo-ovale; fsm, fossa for stapedial muscle; gc, glenoid cavity of scapula; gfm, glenoid fossa of squamosal; gml, groove for mandibular ligament; gs, gingival sulcus; hh, head of humerus; hst, head of stapes; ?i, possible incus; iam, internal acoustic meatus; ifc, internal opening of facial canal; II–V, second-to-fifth digit; inv, involucrum; iof, infraorbital foramen; iop, infraorbital plate of maxilla; isf, infraspinous fossa of scapula; j, jugal; jn, jugular notch; l, lunate; latf, lateral furrow; lc, lambdoidal crest; lep, lenticular process; 2lg, second laminar groove; lmx, lateral process of maxilla; lsc, lateral squamosal crest; lt, lateral tuberosity of periotic; mdc, mandibular condyle; mf, mallear fossa; mfo, mental foramen; mhg, mylohyoidal groove; mrg, mesorostral groove; mt2–5, metacarpals 1–5; mup, muscular process (stapes); mx; maxilla; mxb, lateral border of maxilla; n, nasal; na, neural apophysis; nc, neural channel; nf, narial fossa; nfr-s, nasofrontal suture; o, orbit; oc, occipital condyle; och, optical channel; of, optical foramen; ofh, humerus facet for olecranon process of ulna; oft, open foramen transversarium; opu, olecranon process of ulna; oul, outer lip; ow, oval window; p, parietal; patb, posterior site for attach with periotic; pch, pars cochlearis of periotic; pe, posterior end of the pelvis; per, proximal epiphysis of radius; pg, promontorial groove; pgp, postglenoid process of squamosal; plc, posterolateral corner; plf, perilymphatic duct; pmc, posteromedial corner; pmx, premaxilla; pop, postorbital process of supraorbital process of the frontal; ppp, posterior process of periotic; pppb-br, broken base of posterior process of periotic; p-sq, parietal–squamosal suture; pt, pterygoid; ptg, groove for insertion of pterygoid muscle; ptf, pterygoid fossa; rfh, radial facet of humerus; rw, round window; sc, sagittal crest; sip, sigmoid process; smf, stylomastoid fossa; soc, supraoccipital; sop, supraorbital process of frontal; spf, supraspinous fossa of scapula; sq, squamosal; ss, scapular spine; ssf, subscapular fossa; st, stapes; stfo, stapedial foramen (stapes); ST(T1), scala tympani, first cochlear turn; SV(T1), scala vestibuli, first cochlear turn; T, thoracic vertebra; tc, temporal crest; T2, second cochlear turn; td, trapezoid; tf, temporal fossa; tyc, tympanic cavity; typ, tympanic plate; ufh, ulnar facet of humerus; um, umbo (stapes); un, unciform; V, trigeminal nerve; v, vomer; va, ventral apophysis; vaa, ventral apophysis of atlas; VII-g, groove for facial nerve under the posterior process of the periotic; vk, ventral keel of maxilla; zyg, zygomatic process of squamosal.

Institutional abbreviations: AMNH, American Museum of Natural History, New York, USA; ChM, The Charleston Museum, Charleston, USA; ISAM, IZIKO South African Museum, Cape Town, South Africa; MAUL, Museo dell'Ambiente, University of Lecce, Italy; MCA, Museo Geopaleontologico 'Giuseppe Cortesi', Castell'Arquato, Italy; MGB, Museo Geopaleontologico 'Giovanni Capellini', University of Bologna, Bologna, Italy; MNB, Museum für Naturkunde, Berlin, Germany; MRSN, Museo Regionale di Storia Naturale, University of Torino, Torino, Italy; MSNT, Museo di Storia Naturale e del Territorio, Università di Pisa, Calci, Italy; NMB, Natuurmuseum Brabant, Tilburg, the Netherlands; NMR, Natuurhistorisch Museum, Rotterdam, the Netherlands; RBINS, Royal Belgian Institute of Natural Sciences, Brussels, Belgium; SBAER, Inventory of Superintendency of Cultural Heritage of Emilia Romagna Region, Italy; SMNS, Staatliches Museum für Naturkunde, Stuttgart, Germany; USNM, United States National Museum, Smithsonian Institution, Washington D.C., USA; ZMA, Zoological Museum, Amsterdam, the Netherlands; ZML, Naturalis (Nederlands Centrum voor Biodiversiteit), Leiden, the Netherlands.

SYSTEMATIC PALAEONTOLOGY

CLASS MAMMALIA LINNAEUS, 1758

ORDER CETACEA BRISSON, 1762

SUBORDER MYSTICETI COPE, 1891

CHAEOMYSTICETI MITCHELL, 1989

SUPERFAMILY BALAENOIDEA FLOWER, 1865

FAMILY NEOBALAENIDAE MILLER, 1923

MIOCAPEREA GEN. NOV.

Diagnosis. *Miocaperea* differs from *Caperea* (which is the only other known genus of Neobalaenidae) by: a reduced protrusion of the exoccipital that reaches a point only slightly posterior to the occipital condyles; its temporal fossa, with the squamosal fossa mainly vertical, whereas in the living *Caperea* it is inclined anteroventrally from the lambdoid crest; lambdoid crest triangular, but in *Caperea* it is rounded; the alisphenoid is excluded from being exposed in the temporal fossa, and the foramen pseudo-ovale is completely included within the squamosal, whereas in *Caperea*, the alisphenoid is exposed in the temporal fossa and the foramen pseudo-ovale is located in the pterygoid.

Discussion. Several characters allow us to distinguish SMNS 46978 from the living pygmy right whale *C. marginata*. A comparison of Figures 2 and S1 shows that the whole posterior portion of the skull of *M. pulchra* gen. et sp. nov. is different from the corresponding portion of *C. marginata*. In particular, the extreme posterior projection observed in the latter is totally lacking in the former. The shape of the posterior portion of the temporal fossa, the posterior development of the lambdoid crest, and the orientation of the squamosal fossa result in different arrangements and function of the temporal muscle in the two taxa. Additionally, the shorter posterior protrusion of the exoccipital in *M. pulchra* gen. et sp. nov. suggests a different development of neck muscles. Finally, the different relationships that the foramen pseudo-ovale has with the surrounding bones suggests different developmental paths of the ventrolateral surface of the skull posteriorly to the supraorbital process of the frontal. All these differences support a clear distinction between *C. marginata* and specimen SMNS 46978, the principal subject of this article. Such a distinction is better represented by assigning SMNS 46978 to a different genus, namely *Miocaperea*.

Etymology. *Mio* from Miocene; *Caperea*, scientific name for the pygmy right whale.

MIOCAPEREA PULCHRA SP. NOV.

Holotype. SMNS 46978 of the Palaeontological Collection. The specimen consists of a skull subdivided into two parts: one including the rostrum and the other including the neurocranium. The tympanic bullae are missing.

Type locality. Aguada de Lomas (Sacaco area, Arequipa Department, Peru) is a well-known fossil-bearing site located around 550 km south-east of Lima (Fig. 1) in the Pisco Formation (De Muizon & Bellon, 1981; De Muizon & DeVries, 1985). The locality is close to the southern coast of Peru and its height is around 250–300 m a.s.l. The approximate geographic co-ordinates for the locality are: 15°5′S, 74°8′W.

Formation and age. Pisco Formation. The Pisco Formation outcrop at Aguada de Lomas has been extensively studied (De Muizon & Bellon, 1981; De Muizon & DeVries, 1985; De Muizon *et al*., 2003) because this locality yielded several well-preserved marine vertebrate fossils, including whales and aquatic sloths (De Muizon, 1988; Pilleri, 1989; De Muizon *et al*., 2003). Mollusc and vertebrate biostratigraphies together with radioisotopic dating constrain the age of the sediments to late Tortonian (Late Miocene), 7–8 Mya (De Muizon & Bellon, 1981; De Muizon & DeVries, 1985).

Diagnosis. As for genus.

Etymology. *Pulchra*, Latin, beautiful, referring to the exquisite condition of preservation of the type specimen.

COMPARATIVE ANATOMY

The following descriptions are based on the *M. pulchra* gen. et sp. nov. holotype (SMNS 46978), a skeleton of *C. marginata* on display at RBINS (RBINS 1536), another specimen of *C. marginata* held by AMNH (AMO 36692), five specimens held by ISAM (ZM 41126, ZM 14407, ZM 19944, ZM 40626, 03/06 on display), and one specimen in the private collection of Klaas Post, Urk, the Netherlands. Observations and descriptions, together with several images of the skeleton of *C. Marginata*, are reported in the Supporting information, published online.

PREMAXILLA

In dorsal view, the premaxilla is anteriorly flat and its anterior end extends anterior to the rostral apex of the maxilla (Figs 2, 3; Table 1). Approaching the

narial fossa, the medial border of the premaxilla becomes nearly vertical, and its dorsolateral border becomes dorsally convex. Premaxillary foramina are absent. The posteriormost portion of the premaxilla is developed laterally to the nasal, but its posterior end is more anterior than the posterolateral corner of the nasal, thus the posterolateral portion of the nasal is in contact with the posteromedial part of the maxilla. The narial fossa is relatively enormous (Table 1) and has an oval shape (Figs 2, 3). In lateral view (Figs 2, 3), only the anterior half of the premaxilla is visible and appears scarcely arched. There are no particular differences between the premaxilla of *M. pulchra* gen. et sp. nov. and that of *C. marginata* (Figs S1–S3).

Maxilla

In lateral view (Figs 2, 3), the maxilla is arched but it is not as transversely compressed as that of Balaenidae because its external surface is largely horizontal. Ventrally, the maxilla is concave both transversely and longitudinally. The medial border forms a pronounced ventral keel that is visible when the skull is in lateral view. Unfortunately, the ventromedial border of the maxilla is not preserved continuously, thus the vomer appears along the midline in the posteriormost part of the rostrum in ventral view (Figs 2, 3). Most of the ventral surface of the maxilla is obscured by the baleen and matrix.

Observing *M. pulchra* gen. et sp. nov. in dorsal view, the maxilla is triangular with an outward convex external border (Figs 2, 3). The lateral edge of the bone converges towards the longitudinal axis of the skull, ending only a few millimetres posterior to the anterior end of the premaxilla. The lateral process of the maxilla, which is preserved on the right side of the skull, still in articulation with the supraorbital

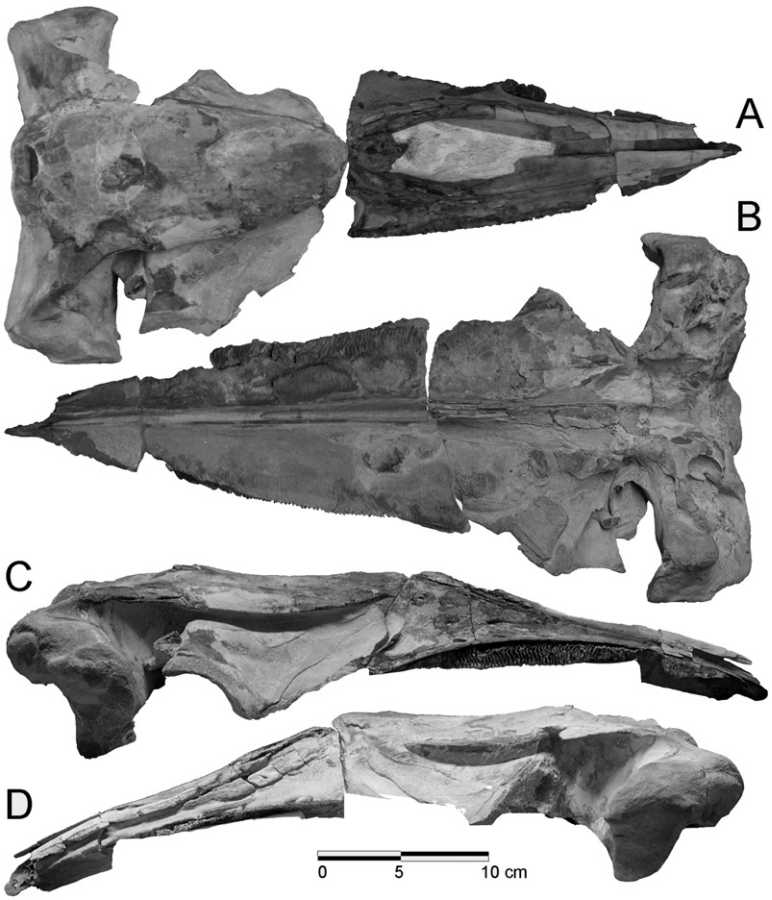

Figure 2. ***Miocaperea pulchra*** **gen. et sp. nov.**: holotype. A, dorsal view; B, ventral view; C, right lateral view; D, left lateral view. In (A) the anterior portion (rostrum) is on the same plane as that on which the neurocranium is lodged, in order to better show the nasal bones. This results in wide gaps between the maxillae and the supraorbital processes of the frontal. Such gaps are absent in (B) because the anterior portion is closer to the neurocranium, to represent the whole skull in articulation.

process of the frontal, projects posteriorly. The infraorbital plate is developed under the anterior portion of the supraorbital process of the frontal from the lateral process of the maxilla. The posterior border of the infraorbital process is broadly rectangular in ventral view, and its posterior border is interrupted by a deep excavation located medially that is interposed between the infraorbital plate and the baleen-bearing portion of the maxilla (Figs 2, 3).

Lateral to the narial fossa, the medial border of the maxilla is raised and its dorsal rim is acutely edged. The surface of the maxilla lateral to this rim is concave (in anterior view; Fig. 4).

There are six infraorbital foramina on the right maxilla and eight on the left maxilla. The infraorbital foramina are filled by hard matrix that forms an endocast of the emergence of the maxillary ramus of the trigeminal nerve (Fig. 5).

In dorsal view, what remains of the posteromedial corner of the maxilla projects posteriorly and medially, but there is no evidence of a long ascending process similar to that observed in Balaenopteridae, Eschrichtiidae, and Cetotheriidae.

The maxilla of *C. marginata* does not show significant differences (Figs S1–S4).

Baleen

Portions of the baleen apparatus are beautifully preserved. On the right side of the rostrum there are

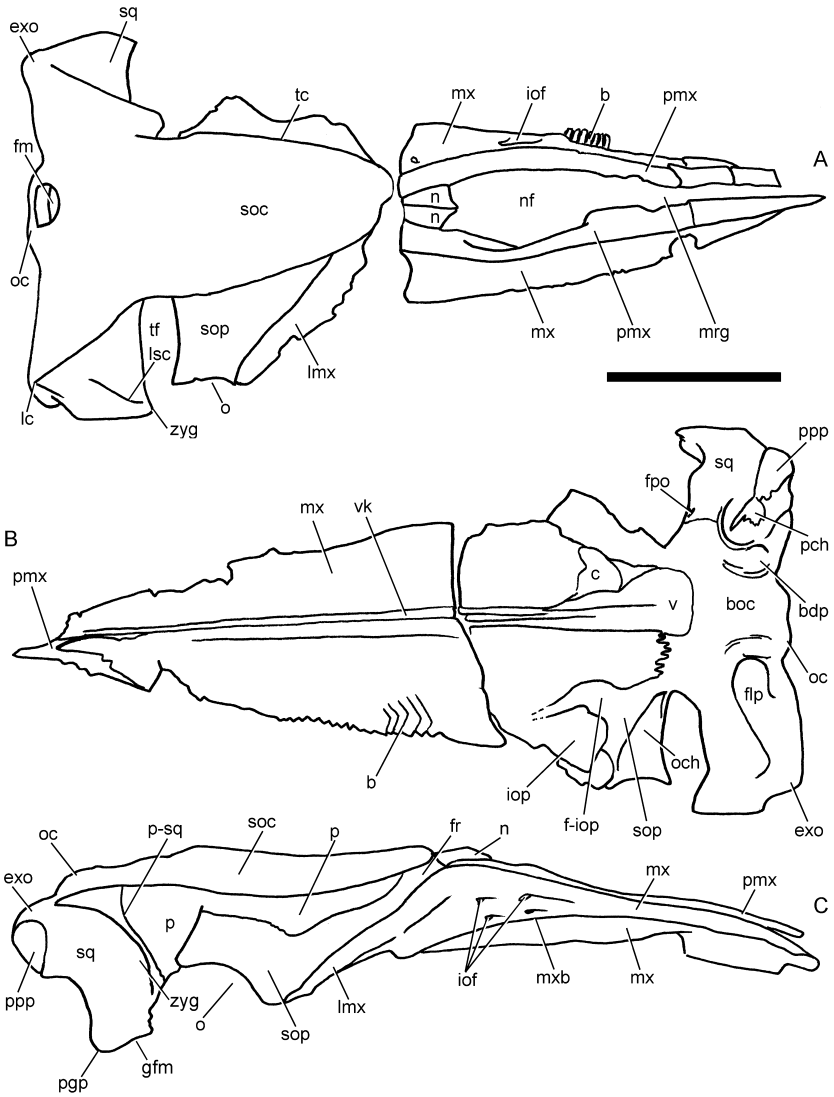

Figure 3. ***Miocaperea pulchra*** **gen. et sp. nov.**: schematic representation of the holotype skull. A, dorsal view; B, ventral view; C, right lateral view. Scale bar: 100 mm. See Anatomical abbreviations for definitions of the acronyms.

Table 1. Skull measurements of Neobalaenidae

Character	***Miocaperea pulchra* gen. et sp. nov.**	*Caperea marginata*				
		ZM 40626	ZM 41126	ZM 14407	RBINS 1536	AMO 36692
Condylobasal length	Anterior piece, 540; posterior piece, 510; estimated total length, 1010	1540	780	760	1360	1370
Maximum width at middle of orbits	–	810	360	–	–	480
Maximum width at zygomatic processes	560	840	389		~800	640
Length of narial fossa	151	–	–	–	–	–
Width of narial fossa	91	–	–	–	–	–
Maximum length of maxilla (medially)	537	–	440	–	–	–
Maximum width of maxilla (up to the external tip of the lateral process)	220	–	225	–	–	–
Maximum length of premaxilla	492	–	–	–	–	–
Maximum width of premaxilla anteriorly to the narial fossa	41	–	–	–	–	–
Maximum width of premaxilla at the middle of narial fossa	18	–	–	–	–	–
Maximum length of interorbital region of the frontal	15	–	–	–	–	–
Nasal length	right, 64; left, 64	–	right, 66; left, 59	–	–	–
Nasal width	right, 27; left, 25	–	right, 16; left, 16	–	–	–
Maximum width of supraorbital process of frontal	145	–	–	–	–	–
Maximum length of supraoccipital	451	–	315	–	605	500
Maximum width of supraoccipital at midlength	210	–	157	–		
Maximum width of supraoccipital between lambdoid crests	465	–	–	–	405	380
Transverse diameter of foramen magnum	60	–	39.65	–	–	45
Longitudinal diameter of foramen magnum	39	–	32	–	–	40.61
Longitudinal diameter of occipital condyle	right, 75; left, 80	–	right, 71.6; left, 67	–	–	–
Transverse diameter of occipital condyle	right, 35; left, 40	–	right, 55; left, 48.8	–	–	–
Maximum distance between external borders of occipital condyles	141	170	135	–	–	–
Transverse distance between the external corners of the exoccipitals	483	–	365	–	–	–
Maximum height of baleen	37 (as preserved)	–	–	–	–	550

Data are listed in mm.

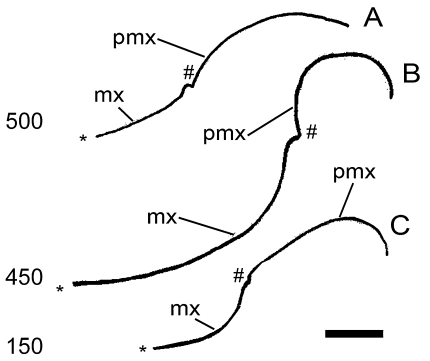

Figure 4. ***Miocaperea pulchra*** **gen. et sp. nov.**: transverse sections of the right side of the rostrum. All sections represent the dorsal surface of the right maxilla and premaxilla. A, posterior section; B, section taken at approximately mid-length of narial fossa; C, anterior section. Numbers on the left refer to the distance (in mm) from the anterior end of the rostrum. Scale bar: 10 mm. *lateral border of maxilla; #premaxilla–maxilla suture.

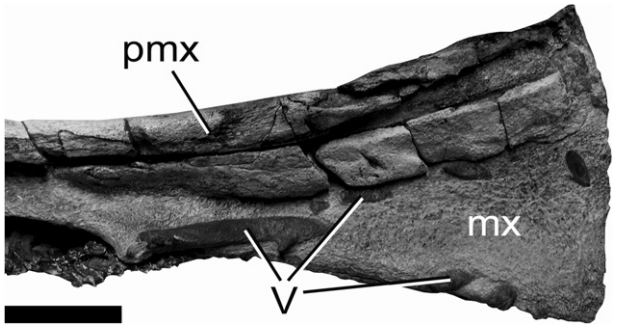

Figure 5. ***Miocaperea pulchra*** **gen. et sp. nov.**: holotype, infraorbital foramina and cast of trigeminal nerve. Scale bars: 50 mm. See Anatomical abbreviations for definitions of the acronyms. Anterior is on the left. Note that hard matrix filled the infraorbital foramina, forming a natural endocast of the exit of the trigeminal nerve (V).

the 'roots' of 111 baleen plates, 53 of which are observed also in lateral view (Fig. 6); the difference in number is likely to result from preservational bias. On the left side, there are the 'roots' of 91 baleen plates in ventral view. The baleen consists of vertical laminae surrounded by matrix that project anteriorly and medially; laterally, they form a ~30° angle with the border of the maxilla. They form a medial posterior concavity and, posteriorly, are surrounded by matrix. Given that the mean density of baleen plates per cm is 2.1, it can be estimated that the total number of baleen plates was around 156 per side. The baleen plates appear permineralized, but as most of them remain within matrix it is difficult to ascertain which kind of fossilization process occurred to preserve them.

It is not possible to obtain an accurate estimation of the length of the baleen because they are broken only a few centimetres from their bases. The maximum height of the baleen, as preserved, is found in the right series, where a small number of laminae are 37 mm in height.

In contrast to *M. pulchra* gen. et sp. nov., the extant *C. marginata* displays a higher number of baleen plates (Fig. 7). According to personal observations on AMO 36692, *C. marginata* has around 220 baleen plates, ~65 more than *M. pulchra* gen. et sp. nov. The number of baleen plates predicted to occur in *M. pulchra* gen. et sp. nov. is in the range of that found for *Eschrichtius robustus* (Lilljeborg, 1861) (Wolman, 1985), but is significantly fewer than that observed in all of the other living mysticete species. See the Supporting information for a description of *C. marginata* baleen.

Nasal

In dorsal view, the nasal shows a concave anterior border in which the medial corner is located more anteriorly than the lateral corner. The lateral border of the nasal projects posteriorly and medially, and terminates only a few millimetres into the interorbital region of the frontal. The anterior border is located more anteriorly than the antorbital corner of the supraorbital process of the frontal. The lateral border of the nasal is in contact with the posterior end of the premaxilla in its anteriormost portion (Figs 2, 3).

The nasal bones of *M. pulchra* gen. et sp. nov. are not distinguishable from those of *C. marginata* (see Supporting information).

Frontal

The supraorbital process of the frontal of *M. pulchra* gen. et sp. nov. is rather short along the transverse axis of the skull (Table 1). It is depressed from the interorbital region, and projects posteriorly and laterally (Figs 2, 3). The supraorbital process of the frontal is not abruptly depressed, as observed in balaenopterids, but neither does it gently descend from the interorbital region of the frontal, as seen in Balaenidae and Cetotheriidae *s.s.* and *s.l.*: its depression is intermediate between the two (see also Marx, 2010 for a discussion on this character). The anterior border projects posterolaterally; the posterior border gently descends ventrally and projects posteriorly

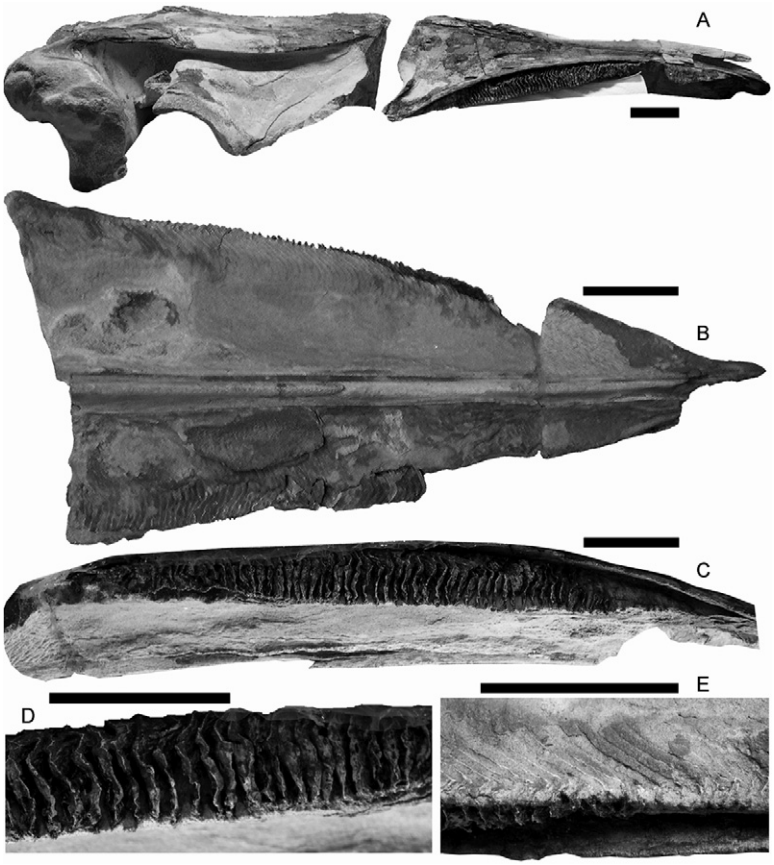

Figure 6. ***Miocaperea pulchra*** **gen. et sp. nov.**: holotype, baleen. A, skull in right lateral view; B, rostrum in ventral view, showing the baleen; C, rostrum in right ventrolateral view, showing the whole baleen series as preserved; D, close-up view of right baleen series in lateral view; E, close-up view of left baleen series in ventrolateral view (ventral is upside). Scale bars: 50 mm.

Figure 7. *Caperea marginata*: specimen AMNH AMO 36692 in right lateral view, showing baleen. Scale bar: 200 mm. The specimen is older than the other specimens represented in Figure S1. Note the angle between the posterior projection of the exoccipital and the dorsal surface of the supraoccipital: this arrangement corresponds to a different geometry of the posterior portion of the skull in the adult individual, with respect to the juveniles of Figure S3.

only slightly. The dorsal surface of the supraorbital process is planar and the ascending temporal crest is absent. The orbit is anteroposteriorly elongated; the antorbital process protrudes laterally more than the triangular and short postorbital corner. On the ventral side of the supraorbital process is a long optic channel that widens distally (Figs 2, 3), resembling the condition observed in Balaenopteridae rather than in Balaenidae, where the anteroposterior diameter of the channel does not change strongly at the lateral end of the process. Medially, the posterior border of the channel forms a posterior concavity and becomes, more distally, high and anteroposteriorly narrow, resembling a delicate crest. A secondary channel intercepts the optic channel close to the orbit projecting anteriorly and medially. The optic channel is localised in the posteriormost portion of the supraorbital process. A small foramen is evident on the roof of the optic channel, 35 mm from the lateral border of the supraorbital process.

The interorbital region of the frontal is almost totally hidden by the superimposing supraoccipital: only a short portion of frontal is present, surrounding the posterolateral portion of the nasals. Such a portion is interposed between the supraoccipital, maxilla, premaxilla, and nasal (Figs 2, 3).

There are no significant differences in the shape of the supraorbital process of the frontal of *M. pulchra* gen. et sp. nov. with respect to that of *C. marginata* (Supporting information).

Lacrimal

As in *C. marginata*, the lacrimal is elongated and transversely narrow (Figs 2, 3). It is in close contact with the anterolateral corner of the supraorbital process. It does not show distinctive morphological features.

Jugal and interparietal

The jugal is missing. No trace of an interparietal was found in the holotype specimen, and thus such a bone is considered to be absent. The jugal of *C. marginata* is described in the Supporting information. The interparietal is absent in *C. marginata* (see Supporting information).

Parietal

In lateral view (Figs 2, 3), the anterior portion of the parietal is dorsoventrally compressed. The frontal border is straight and projects dorsally and anteriorly. Further posteriorly, the frontal border is partially superimposed on the medial portion of the supraorbital process of the frontal; articular grooves on the posteromedial part of the supraorbital process suggest that the parietal was much more extended laterally than can be observed now. In dorsal view (Figs 2, 3) the parietal is not exposed at the vertex because the external occipital protuberance of the supraoccipital is superimposed on it. Posteriorly to the posterior border of the supraorbital process, the parietal widens dorsoventrally, forming the medial wall of the temporal fossa. The dorsal border contributes to the formation of the dorsal attachment line of the temporal muscle together with the lateral border of the supraoccipital; this line, corresponding to the temporal crest, protrudes laterally and overwhelms the temporal fossa, which cannot thus be observed in dorsal view. The parietal–squamosal suture shows a slight anterior concavity and terminates, dorsally, at a point localized on the parietal–squamosal–supraoccipital interface, which is slightly anterior to the posterior apex of the lambdoid crest (Fig. 8).

The parietal of *C. marginata* does not show particular differences. The level of superimposition of the parietal on the supraorbital process of the frontal may vary, depending on individual variation and, possibly, on age (see the Supporting information for a full description of this bone in *C. marginata*). The parietal–squamosal suture projects further posterodorsally than in *M. pulchra* gen. et sp. nov., and does not show any sign of anterior concavity. This is probably related to the different geometry of the posterior part of the temporal fossa that distinguish *M. pulchra* gen. et sp. nov. and *C. marginata*.

Vertex

The skull vertex of *M. pulchra* gen. et sp. nov. shows the same characters observed in *C. marginata* (Figs 2, 3). What remains of the posteromedial corners of the maxillae obliterates part of the interorbital region of the frontal, which is only exposed posterior and lateral to the nasals. The supraoccipital is superimposed on the parietal and on the posterior portion of the interorbital region of the frontal, therefore the parietal is excluded from the skull vertex.

In *C. marginata*, ontogenetic variation includes the superimposition of the supraoccipital on the posterior end of the maxillae and a variable range of exposure of the interorbital region of the frontal at the cranial vertex (Fig. 9). In juvenile individuals the posterior ends of the maxillae are located further anteriorly than the anterior border of the supraoccipital; in older individuals the supraoccipital is superimposed on them, obliterating the view of these elements from a dorsal viewpoint. The parietal is not exposed at the cranial vertex and is instead covered by the supraoccipital.

Squamosal

Typical features of the squamosal of Neobalaenidae include a massive reduction of the zygomatic process and a strong ventral protrusion of the postglenoid process. Both these features are observed in *M. pulchra* gen. et sp. nov. (Figs 2, 3). In this species the zygomatic process is round and short. There is a considerable distance between the zygomatic process and the postglenoid process along the dorsoventral axis. In lateral view, the postglenoid process projects ventrally and has a rounded ventral border. Its posterior border forms a wide concavity, which terminates at the anteroventral crest of the attach site for the posterior process of the periotic. The glenoid cavity of the squamosal is localized along a surface included between the anterodorsal zygomatic process and the posteroventral postglenoid process. Given

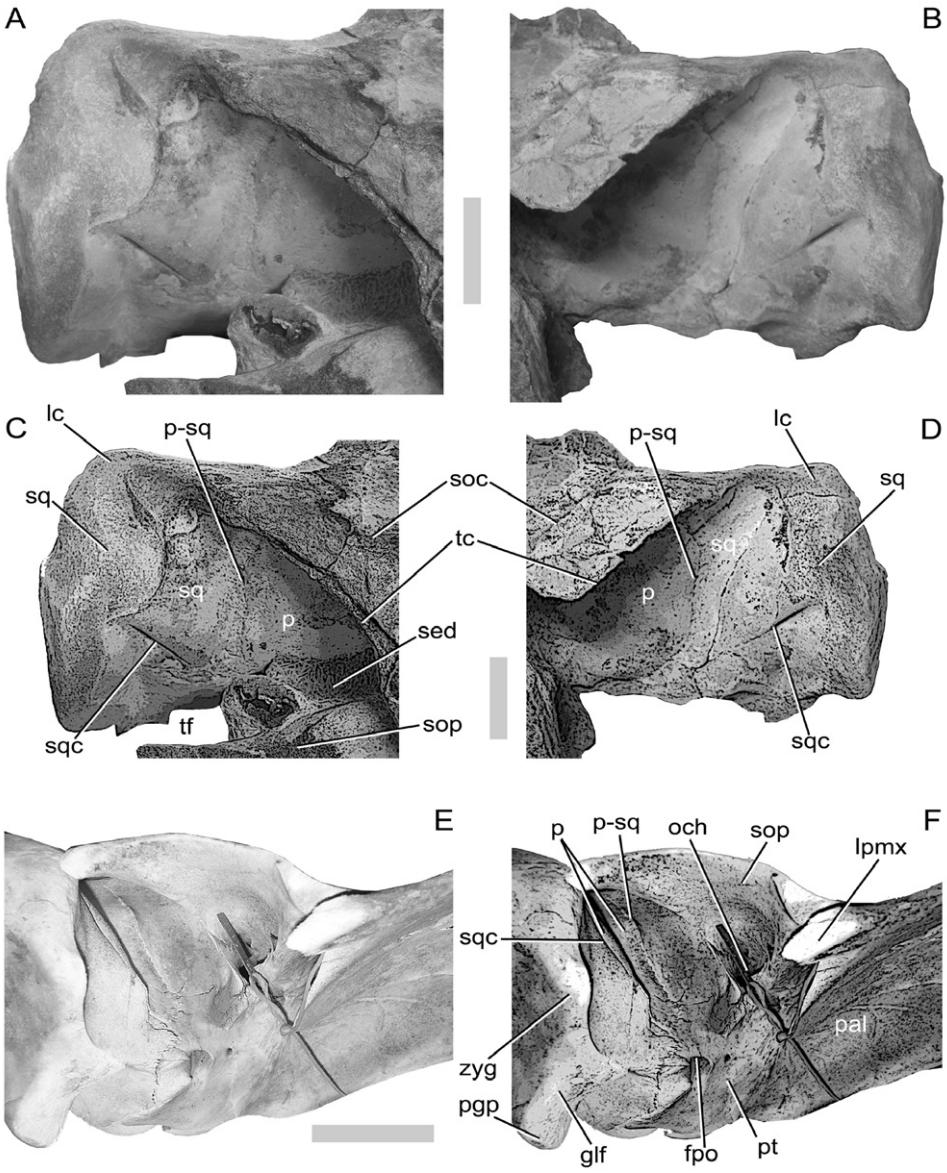

Figure 8. Schematic representation of the structure of the temporal fossa in Neobalaenidae. A, ***Miocaperea pulchra* gen. et sp. nov.**, right squamosal in anterodorsal view; B, ***M. pulchra* gen. et sp. nov.**, left squamosal in anterodorsal view; C, ***M. pulchra* gen. et sp. nov.**, sketch of right squamosal in anterodorsal view; D, ***M. pulchra* gen. et sp. nov.**, sketch of left squamosal in anterodorsal view; E, *Caperea marginata* (ZM 41126), right temporal fossa in ventrolateral view; F, *C. marginata* (ZM 41126), sketch of right temporal fossa in ventrolateral view. Scale bars: 50 mm. See Anatomical abbreviations for definitions of the acronyms.

this localization, the anteriormost part of the glenoid fossa of the squamosal is positioned ventral and slightly posterior to the orbit.

In dorsal view, the squamosal fossa of the temporal fossa is perpendicular to the longitudinal axis of the skull (Figs 2, 3). It is anteromedially bordered by the parietal–squamosal suture, which is anteriorly concave; it is also dorsally bordered by the lambdoid crest, which is the posterior prolongation of the temporal crest. Posteriorly, the lambdoid crest forms a triangular apex that reaches a point only slightly posterior to the occipital condyles. Anterior to the posterior apex of the lambdoid crest the squamosal fossa is horizontal for a few centimeters, after which it becomes vertical. Transversely, the squamosal fossa is slightly convex in dorsal view.

A straight squamosal cleft emerges from the parietal–squamosal suture and projects laterally and

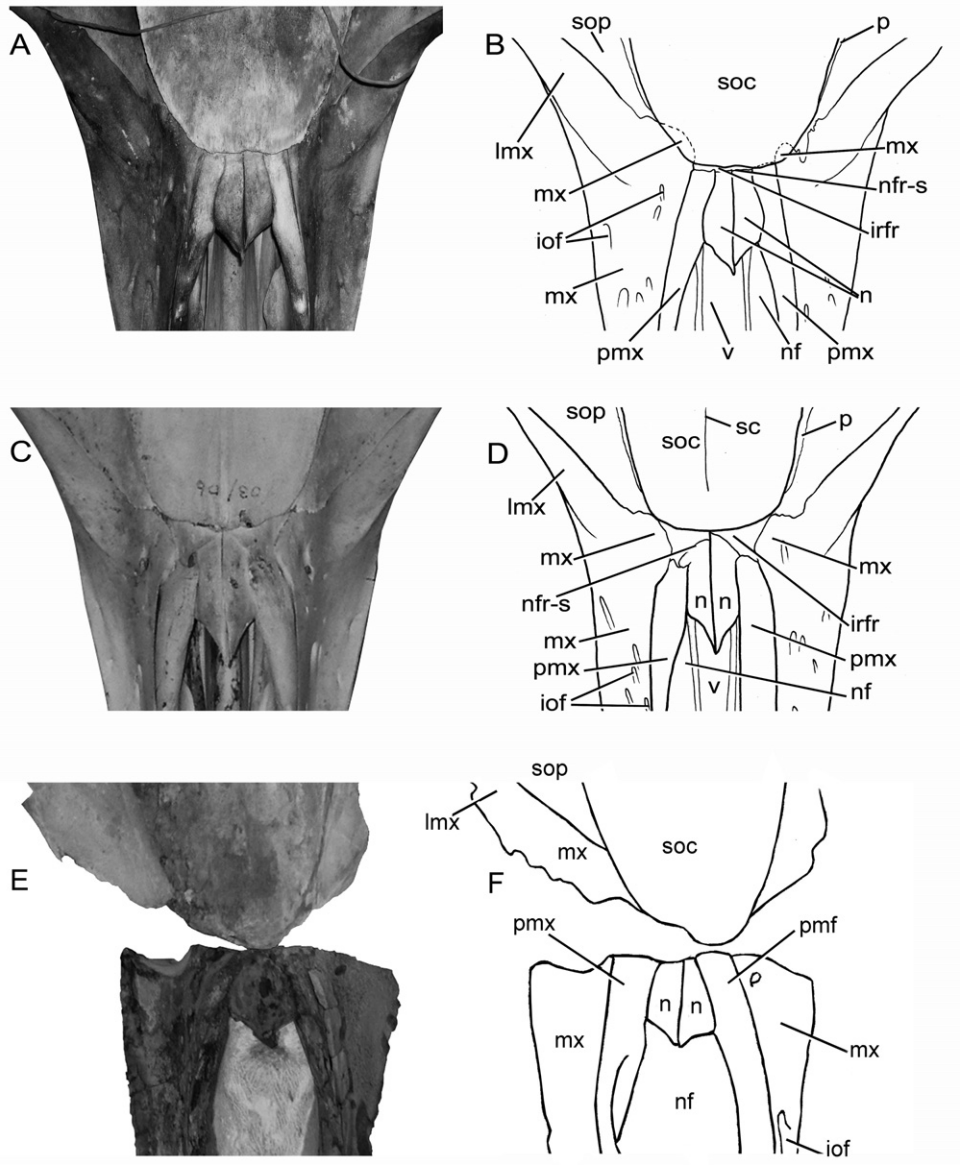

Figure 9. Vertex of Neobalaenidae. A, B, *Caperea marginata* specimen ISAM ZM 41126, a possibile young adult; C, D, *Caperea marginata* specimen ISAM 03/06 (on display), a juvenile (not newborn) individual. E, F, ***Miocaperea pulchra* gen. et sp. nov.** (holotype), reconstruction of vertex. Not to scale. See Anatomical abbreviations for definitions of the acronyms. Note that in the living *C. marginata*, the bone arrangement at the cranial vertex differs in relation to the age of the individuals. In fact, in the young adult individual the interorbital region of the frontal is reduced to an anteroposteriorly compressed portion, but in the juvenile this region is further expanded. Moreover, in the adult individual, the posteromedial corners of the maxilla are located under the supraoccipital, but in the juvenile they are separated from it.

dorsally; its distal end curves ventrally and terminates at a position close to the zygomatic process of the squamosal (Fig. 8). Ventrally, the parietal–squamosal suture contacts the dorsal border of the pterygoid and the vomer. There is no contact between squamosal, parietal, and alisphenoid on the external surface of the skull, as the alisphenoid is not exposed. The absence of the alisphenoid from the lateral side of the skull depends on the fact that it is covered by the surrounding bones.

Anteroventrally, the falciform process of the squamosal is perforated by a rather large foramen pseudo-ovale (Table 1) that bears dorsal and ventral fissures (Fig. 10).

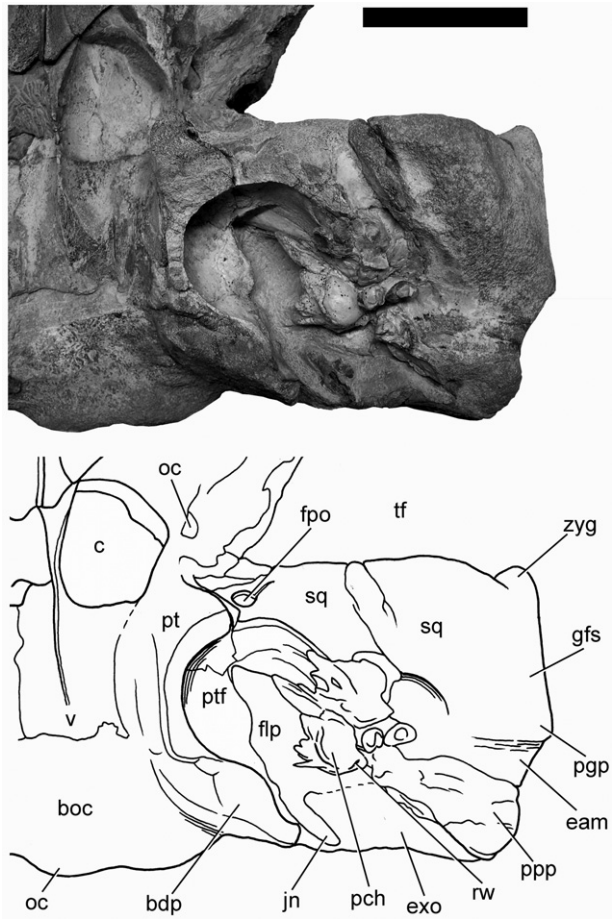

Figure 10. ***Miocaperea pulchra*** **gen. et sp. nov.**: holotype, basicranium, left side. A, holotype skull; B, schematic representation. Scale bars: 50 mm. See Anatomical abbreviations for definitions of the acronyms.

On the lateral side of the squamosal, the lateral squamosal crest appears rounded and scarcely developed, and there are no signs of fossae for the attachment of neck muscles.

In ventral view, the postglenoid process of the squamosal is separated from the pterygoid fossa by a narrow (the maximum thickness is 16 mm) and oblique stripe projecting medially, formed by the squamosal. Such a concave stripe widens in a large external acoustic meatus located much further dorsally than the ventral termination of the postglenoid process. The external acoustic meatus is anteriorly bordered by the posterior border of the postglenoid process; it is dorsally bordered by the squamosal and is posteriorly delimited by the posterior process of the periotic. The postglenoid process appears smaller on the left side and more robust on the right side.

A complete description of the squamosal of *C. marginata* is provided in the Supporting information. Here, it is sufficient to emphasize that in *C. marginata* the posterodorsal part of the bone projects much further posteriorly than in *M. pulchra* gen. et sp. nov., the parietal–squamosal suture are differently shaped (see Parietal, above), the lambdoid crest is wider and rounder in the living species, and is triangular in *M. pulchra* gen. et sp. nov., where its posterior apex is located at the same level as the occipital condyle or anterior to it.

Temporal fossa

Miocaperea pulchra gen. et sp. nov. and *C. marginata* differ fundamentally because of the different shapes of their temporal fossa. In *M. pulchra* gen. et sp. nov. the temporal fossa can be easily observed in dorsal view, as the anterior surface of the squamosal (corresponding to the posterior wall of the temporal fossa) is flat and does not protrude anteroventrally. For this reason, in dorsal view, it is possible to observe the clear, triangular separation between the anterior surface of the squamosal and the posterior border of the supraorbital process of the frontal. In *C. marginata* such a separation cannot be observed because the anterior surface of the squamosal projects anteroventrally, and is inclined from a posterodorsal point to an anteroventral point (in lateral view); therefore, a dorsoventral window is not observed in the temporal fossa of *C. marginata*.

As shown in the Supporting information, however, this character may vary because of age. In younger individuals, a very small dorsoventral window is observed, but such an opening will disappear with growth as the individual approaches adulthood (see Supporting information).

In dorsal view, in *M. pulchra* gen. et sp. nov. the lambdoid crest is located on a transverse line crossing the anterior half of the foramen magnum. In this sense, it is not highly protruded posteriorly. This is another important difference with *C. marginata*. In fact, in the living species, the posterior apex of the lambdoid crest is located much further posteriorly than the foramen magnum and the occipital condyles (see also Baker, 1985 and Supporting information). The posterior projection of the temporal crest and the posterior location of the lambdoid crest are exclusive to *C. marginata*, and are not seen in *M. pulchra* gen. et sp. nov.

In conclusion, it appears that the whole geometry of the temporal fossa of *M. pulchra* gen. et sp. nov. is different from that of *C. marginata*. Orientation of the anterior surface of the squamosal, presence/absence of a dorsoventral opening in the temporal fossa, and relative position of the lambdoid crest are the characters that allow the clear distinction between *M. pulchra* gen. et sp. nov. and *C. marginata*.

Occipital region

The supraoccipital is very elongated and projects anteriorly to superimpose on the posterior part of the interorbital region of the frontal (Figs 2, 3). Its anterior border is narrow and round. The lateral border is lower than the central portion; in dorsal view, the lateral border is externally convex and protrudes laterally, overhanging the medial wall of the temporal fossa and the emergence of the supraorbital process of the frontal. The strong anterior thrust of the supraoccipital prevents the parietal from being exposed at the skull vertex. The anteriormost portion of the supraoccipital reaches a point in close proximity with the posteromedial corner of the maxilla. A longitudinal relief is present in the anterior half of the bone; such a relief becomes flat further posteriorly. However, as the posterior area is largely damaged, it is difficult to be sure about the development of this relief.

The transverse elongation of the exoccipital is relatively large, even enormous. The externally rounded exoccipital is separated from the foramen magnum by the interposition of a deep jugular notch, which is located lateral to the descending process of the basioccipital. Such a process forms the medial border of the foramen lacerus posterius. The occipital condyles are well separated dorsally, but are in close contact ventrally (Fig. 11). The condyles are rectangular and mostly flat. There are no condyloid foramina. The foramen magnum is transversely wide but dorsoventrally compressed. In ventral view, the exoccipital is only slightly visible. Its posterolateral corner is located far from the postglenoid process of the squamosal, and is slightly more medial than the zygomatic process of the squamosal. Such a corner reaches a point located a little more posteriorly than the articular surface of the occipital condyle. The exoccipital forms the posterolateral border of the foramen lacerus posterius, and is in contact with the posterior process of the periotic (Fig. 10).

The ventral surface of the basioccipital is longitudinally convex and transversely concave. The lateral border of the basioccipital forms a wide concavity as it approaches the pterygoid. The descending process of the basioccipital is wide and flat, and terminates ventrally with an acute apex. The jugular notch is rather narrow and long.

The supraoccipital of *C. marginata* is described in the Supporting information. It differs from that of *M. pulchra* gen. et sp. nov. in that its lateral borders are mainly concave, whereas those of *M. pulchra* gen. et sp. nov. are more convex; moreover, in *M. pulchra* gen. et sp. nov. the posterolateral corner of the supraoccipital projects laterally rather abruptly, but in *C. marginata* it is not possible to observe a clear posterolateral corner, as the lateral border of the supraoccipital projects posterolaterally towards the posterior apex of the lambdoid crest.

Alisphenoid

In the temporal fossa the alisphenoid is not exposed, therefore it cannot be described.

In *C. marginata*, the alisphenoid was observed in the temporal fossa of ISAM ZM 14407 and ISAM ZM 41126. In both specimens it was situated

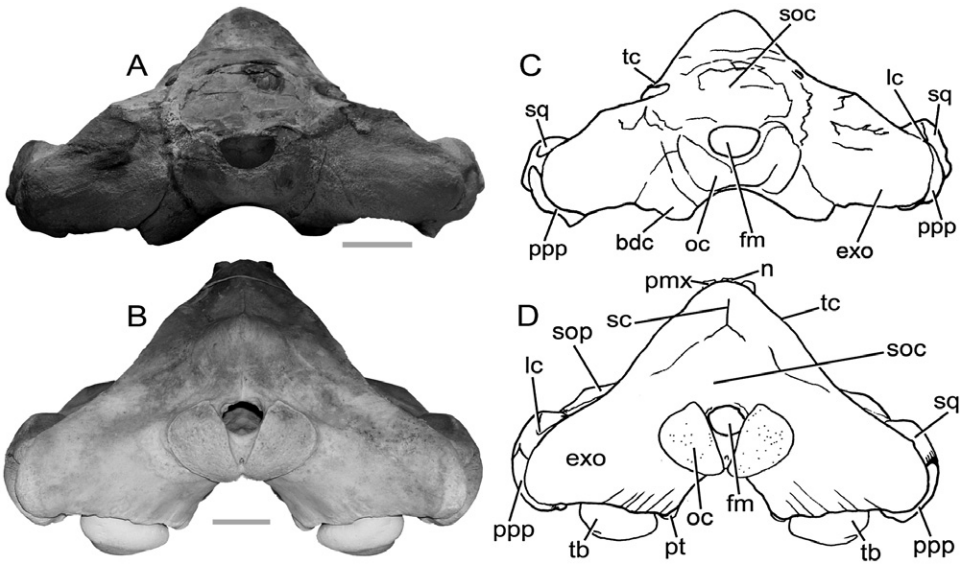

Figure 11. Skull in posterior view. A, ***Miocaperea pulchra* gen. et sp. nov.**; B, *Caperea marginata* (specimen ZM 41126). Scale bars: 100 mm. See Anatomical abbreviations for definitions of the acronyms.

between the parietal (dorsally) and the pterygoid (ventrally and posteriorly). In ISAM ZM 14407, the alisphenoid is a short and narrow stripe with concave ventral border and convex dorsal border. The posterior border is straight and its posterodorsal and posteroventral corners form, respectively, a right and an acute angle with the dorsal and the ventral borders. In ISAM ZM 41126, the alisphonoid is half-moon shaped. Its dorsal border is concave and its ventral border is convex; the posterior border is reduced to a single point located within the parietal. In both specimens the pterygoid is interposed between the alisphenoid and the squamosal.

Pterygoid

The ventral border of the pterygoid is largely eroded; the pterygoid fossa is exposed on the ventral side of the skull because of post-mortem demolition of the posterior part of the palatine.

The pterygoid fossa is widely circular in outline; the roof of the fossa is localized medially. The fossa shows a transverse constriction at around mid-length; in this way, the fossa is formed by two distinct fossae separated by such a constriction. The roof of the anterior part of the fossa ends posteriorly by producing a crest that is posteriorly concave and that shows a posteromedial foramen (Fig. 10). In ventromedial view, the pterygoid projects dorsally and posteriorly, and is dorsally bordered by the falciform process of the squamosal that is interposed between the pterygoid and the foramen pseudo-ovale.

In *C. marginata*, the pterygoid is evident in the anteroventral surface of the temporal fossa. It is dorsally bounded by the parietal and the squamosal in AMNH AMO 36692, ISAM ZM 40626, and RBINS 1536; it is dorsally delimited by the alisphenoid, parietal, and squamosal in ISAM ZM 41126 and ISAM ZM 14407 (Fig. 12). Slightly ventral to the squamosal–parietal–pterygoid suture is the foramen pseudo-ovale, which is completely included within the pterygoid. It may show dorsal and ventral fissures (in ZM 41126 and ZM 40626 the foramen shows a dorsal fissure; in AMNH AMO 36692 the foramen shows both dorsal and ventral fissures).

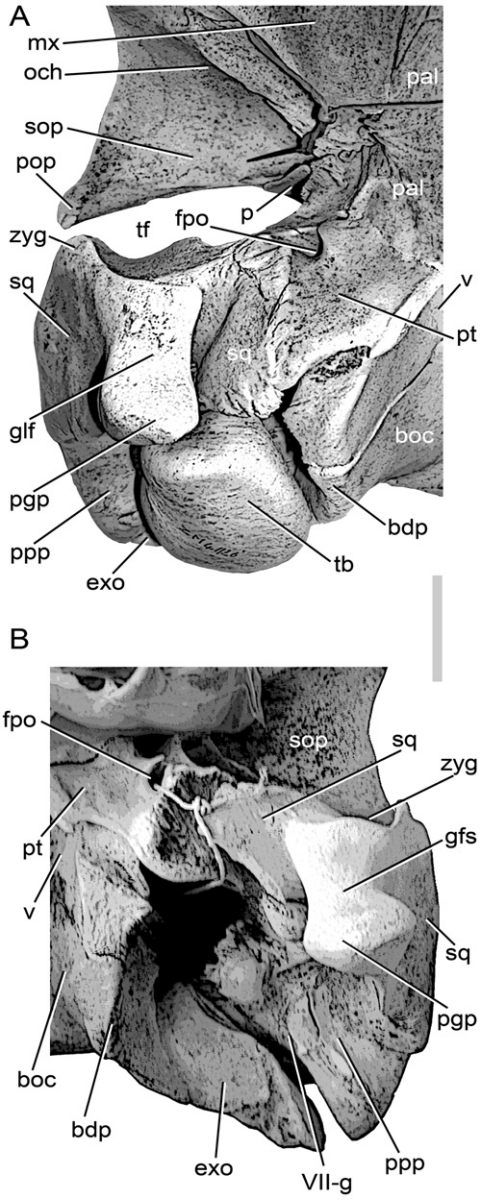

Figure 12. *Caperea marginata*: basicranium. A, right side (specimen ZM 41126) with tympanic bulla *in situ*; B, left side (same specimen), tympanic bulla removed, periotic *in situ*. Scale bar: 100 mm. See Anatomical abbreviations for definitions of the acronyms.

Foramen lacerus posterius

The foramen lacerus posterius is a narrow cavity that is elongated along the anteroposterior axis (Fig. 10). Its medial border is represented by the lateral surface of the descending process of the basioccipital, its lateral border is occupied by the periotic, its posterior border is the anteroventral border of the exoccipital and the jugular notch, and its anterior border is formed by the posterior crest present in the pterygoid fossa. Both the anterior and posterior extremities of the foramen are pointed and triangular. Currently it is filled by the matrix, and lodges the periotics.

In *C. marginata*, the foramen lacerus posterius was not fully available for close inspection in the specimens examined for this study. In all cases it was covered by the presence of tympanic bullae, or it was in part obliterated by the periotic. In Figure 12 a close-up view of the right foramen lacerus posterius of

C. marginata is shown that also includes the periotic. As it can be judged from the illustration, the foramen lacerus posterius is rather wide and squarish in outline; however, the periotic obliterates most of the lateral border, making it impossible to get a full description. From Figure 12 the presence of a wide external acoustic meatus can be recorded.

Palatine

Missing. See Supporting information for a description of the palatine of *C. marginata*.

Vomer

A narrow exposure of the vomer appears in between the medial borders of the maxilla in the posterior portion of the rostrum. Further posteriorly, the vomerine crest is short and disappears slightly anteriorly to the posterior border of the vomer. As in other mysticetes, the posterior surface of the vomer is rather flat and covers the suture between basisphenoid and basioccipital. The vomer is laterally bordered by the pterygoid. Posteriorly, it is bordered by the basioccipital. The vomer of *M. pulchra* gen. et sp. nov. does not seem to show particular differences with respect to that of *C. marginata*. However, a full description of the vomer in the extant *C. marginata* is provided in the Supporting information.

Periotic

The posterior process of the periotic is distally wide; it is ventrally interposed between exoccipital and squamosal, and can be easily observed in lateral and posterior views (Figs 3, 11). The posterior process is flat-to-slightly convex and, distally, is robust and laterally convex. The posterior pedicle for the tympanic bulla is located medially in close proximity to the strong constriction at the base of the posterior process (Fig. 10). Posterior and medial to the posterior pedicle is a posteromedial concavity for the transit of the facial nerve (VII cranial nerve); this concavity is triangular in shape and widens sharply. Measurements of the periotic are provided in Table 2.

The posterior end of the anterior process is difficult to differentiate because it forms the anterolateral border of the pterygoid fossa, and because it is tightly inserted in the skull. A lateral projection of the anterior process is lacking. The anterior apex of the anterior process is triangular with rounded apex; the lateral border of the anterior process is convex, but the medial border is irregularly shaped. A posteromedial spine projects medially into the foramen lacerus posterius from the posteromedial border of the anterior process.

The pars cochlearis (Fig. 13) is ventrally rounded; the promontorial groove is deep, and develops along the anteroposterior axis on the ventral surface of the pars cochlearis. The pars cochlearis is transversely and anteroposteriorly short, and does not protrude into the foramen lacerus posterius. Its ventromedial border is irregularly shaped. The round window is wide (Table 2). The caudal process is squared and does not protrude very much compared with, for instance, balaenopterids. The tensor tympani groove is present and terminates medially slightly posterior to the posteromedial spine of the anterior process. It is not possible to observe the arrangement of the endocranial foramina because they are still immersed in the matrix. The oval window is obliterated by the stapes, which is in contact with the incus; both ossicles cover part of the laterodorsal surface of the periotic.

The pars cochlearis of the right periotic is partially destroyed, and thus part of the cochlea is exposed. A cast of the cochlear turns can be observed (Fig. 13). The cast shows the scala tympani and the scala vestibuli of the first cochlear turn subdivided by the second laminar groove (according to Geisler & Luo, 1996). The second turn of the cochlear canal is visible in part and is separated from the first turn by an evident gap. This pattern is also observed in other mysticetes investigated for cochlear structure (Fleischer, 1976; Geisler & Luo, 1996).

Stapes are still in articulation in both periotics. In *C. marginata*, periotics were studied in detail in ISAM ZM 19944 and in a specimen in the private collection of Klaas Post, Urk, the Netherlands. The posterior process is very massive and robust. It is exposed in the lateral side of the skull, ventral to the exoccipital (Fig. 12). It is included within a tube-shaped articular surface formed by the ventral side of the exoccipital and the posterior face of the squamosal.

A triangular and strong lateral tuberosity is developed posteriorly to the anterior end of the periotic that protrudes laterally. Posterior and medial to the tuberosity the dorsal surface of the periotic is concave.

The morphology of the pars cochlearis and the arrangement of the endocranial foramina represent unique characteristics of *C. marginata* (Fig. 14). The pars cochlearis is ventrally and laterally rounded, but its medial edge is thin and crest-like. The endocranial opening of the facial canal is separated from the internal acoustic meatus by a wide crista transversa. The facial canal is prolonged into a short channel directed towards the anterior part of the rim of the internal acoustic meatus. The internal acoustic meatus is oval in shape, and is located further ventrally than the endocranial opening of the facial

Table 2. Measurements of periotic and tympanic bulla in Neobalaenidae

Character	***Miocaperea pulchra* gen. et sp. nov.** left	*Caperea marginata*		
		ZM 19944 right	ZM 19944 left	Private collection
Periotic				
Length of posterior process	116.2			68
Maximum width of posterior process	62			46
Minimum width of posterior process	22			24
Dorsoventral diameter of internal acoustic meatus		6.95	7.3	6
Anteroposterior diameter of internal acoustic meatus		6.45	6	7
Maximum diameter of oval window	9	8.8	9.5	7
Minimum diameter of oval window	6.1	5	5.3	4
Maximum diameter of round window	–	7.5	7.9	7.5
Minimum diameter of round window	–	6	5.7	6
Maximum diameter of internal opening of the facial canal	–	4	4	4
Minimum diameter of internal opening of the facial canal	–	3	3.9	3.5
Maximum diameter of endolymphatic canal	–	4	2.7	8
Minimum diameter of endolymphatic canal	–	2.75	2.65	1
Maximum diameter of perilymphatic canal	–	4	5.25	2
Minimum diameter of perilymphatic canal	–	1.95	1.8	2
Anteroposterior diameter of pars cochlearis	34	36.5	33	–
Lateromedial diameter of pars cochlearis	41	20	21.6	–
Tympanic bulla	–	–	–	–
Maximum length	–	122.5	123.45	103.6
Posterior width	–	–	–	42
Width at midlength	–	74	71.9	69
Anterior width	–	40		62
Width at sigmoid process	–	81	81	73.6
Height at conical process	–	–	50	45
Height at sigmoid process	–	–	–	70
Height of tympanic cavity	–	39	40	37
Mean thickness	–	3.8	–	5.5
Length of malleus	–	–	39	25
Length of stapes	8	–	10	8
Length of incus	?17.6	–	11	–

Data in mm.

canal. Both the internal acoustic meatus and the facial canal are located on a surface that, in dorsal view, is inclined anterolaterally to posteroventrally. The posterior rim of the internal acoustic meatus is separated from the posteriormost part of the pars cochlearis by a strong dorsoventral crest that is triangular in posterior view. Posterior to this crest, a small endolymphatic duct and a wide perilymphatic duct are open. The round window is wide (Table 2) and is separated from the perilymphatic opening. The stylomastoid fossa is prolonged on the posterior face of the pars cochlearis, dorsal to the round window. A series of median promontorial grooves are present under the internal acoustic meatus; these are also observed in ventral view. In lateral view, the oval window is wide and is separated from the lateral opening of the facial canal by a crest. The caudal process is rather thin and triangular in posterior view. It forms the ventral side of the stapedial muscle fossa that is strongly concave, and is separated from the channel for the facial nerve by a crest. The fossa for the malleus is small and difficult to circumscribe. No ornamental crests resembling those of *M. pulchra* gen. et sp. nov. are observed in the periotic of the extant *C. marginata*, with the exception of a dorsal and triangular crest clearly evident posterodorsal to the internal acoustic meatus, in the same position of the long ornamental crest observed in *M. pulchra* gen. et sp. nov. Measurements of the periotics studied are provided in Table 2.

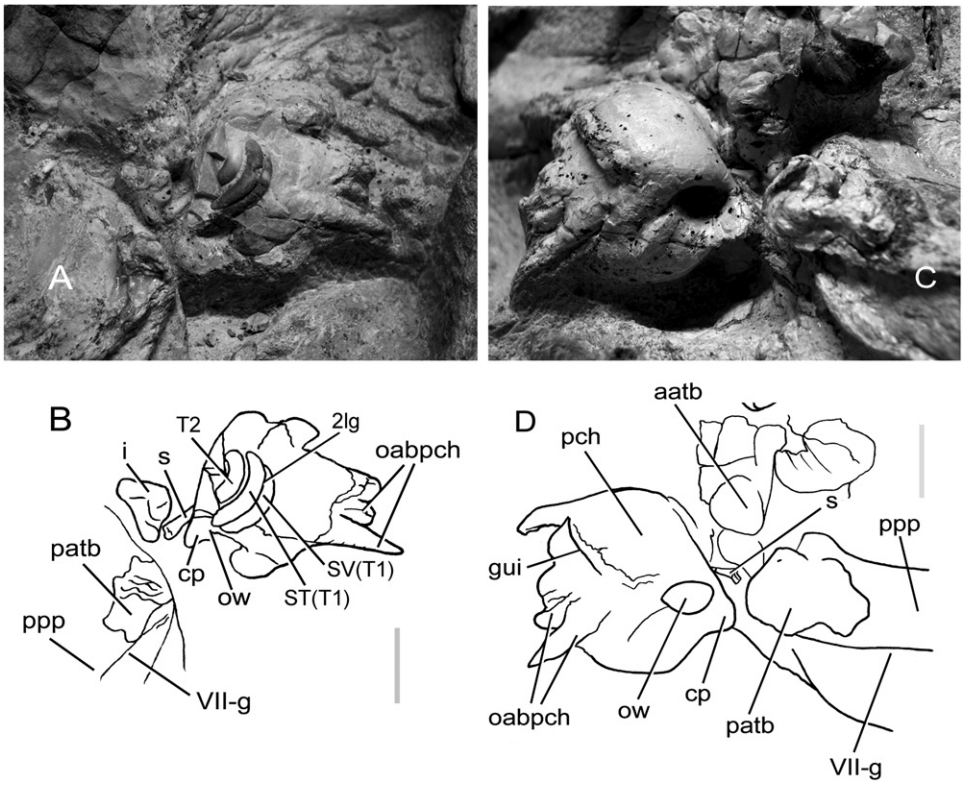

Figure 13. ***Miocaperea pulchra*** **gen. et sp. nov.**: left and right periotics *in situ*. A, B, right periotic; C, D, left periotic. Scale bar: 20 mm. See Anatomical abbreviations for definitions of the acronyms.

Auditory ossicles

Both stapes are in articulation with the periotics, and therefore their footplates cannot be described (Fig. 15). The stapes is elongated (Table 2) and narrow. The head of the stapes seems broadly triangular and appears crossed by a narrow crest (Fig. 15).

It is not clear if a small bone located lateral to the right stapes actually represents the incus (Fig. 15: ?i). The morphology of this small element differs greatly from the incus of the extant *C. marginata*. Additional preparation of the specimen is necessary to fully understand the morphology of this element.

The malleus is missing.

Auditory ossicles of the extant *C. marginata* were studied in specimen ISAM ZM 19944 and in a specimen in the private collection of Klaas Post, Urk, the Netherlands.

One of the two mallea studied in this work was still attached to the sigmoid process of the relative tympanic bulla; the other was detached from the bulla (Fig. 16). In the malleus of *C. marginata* the sulcusfor the chorda tympani is deep and marked, and the obscured lateral foramen for the chorda tympani is profound. The tubercule is distinctly subdivided into two eminences, one of which bears the insertion of tendon for tensor tympani muscle. The anterior process is long and develops in close connection with the sigmoid process. The facets for the incus are rather flat and perpendicular to each other.

The incus is short and stocky (Fig. 16). The articular facet for malleus is scarcely concave; the crus breve is short and pointed; the lenticular process is oval in shape and rather large. The body of the incus is transversely wide at the incudomallear joint, and becomes narrower approaching the lenticular process.

The stapes is short (Table 2); the stapedial foramen is truly perforated (Fig. 16); it is small and located within a triangular fossa. The lateral border of the footplate of the stapes is raised relative to its medial portion; the footplate is oval in shape and relatively enormous, as required by the large extension of the oval window. The articular facet for contact with the incus is relieved and convex in lateral view.

Tympanic bulla

Missing. A description of the tympanic bulla of *C. marginata* is presented in the Supporting information; additional observations are presented in the Discussion (see also Fig. 20).

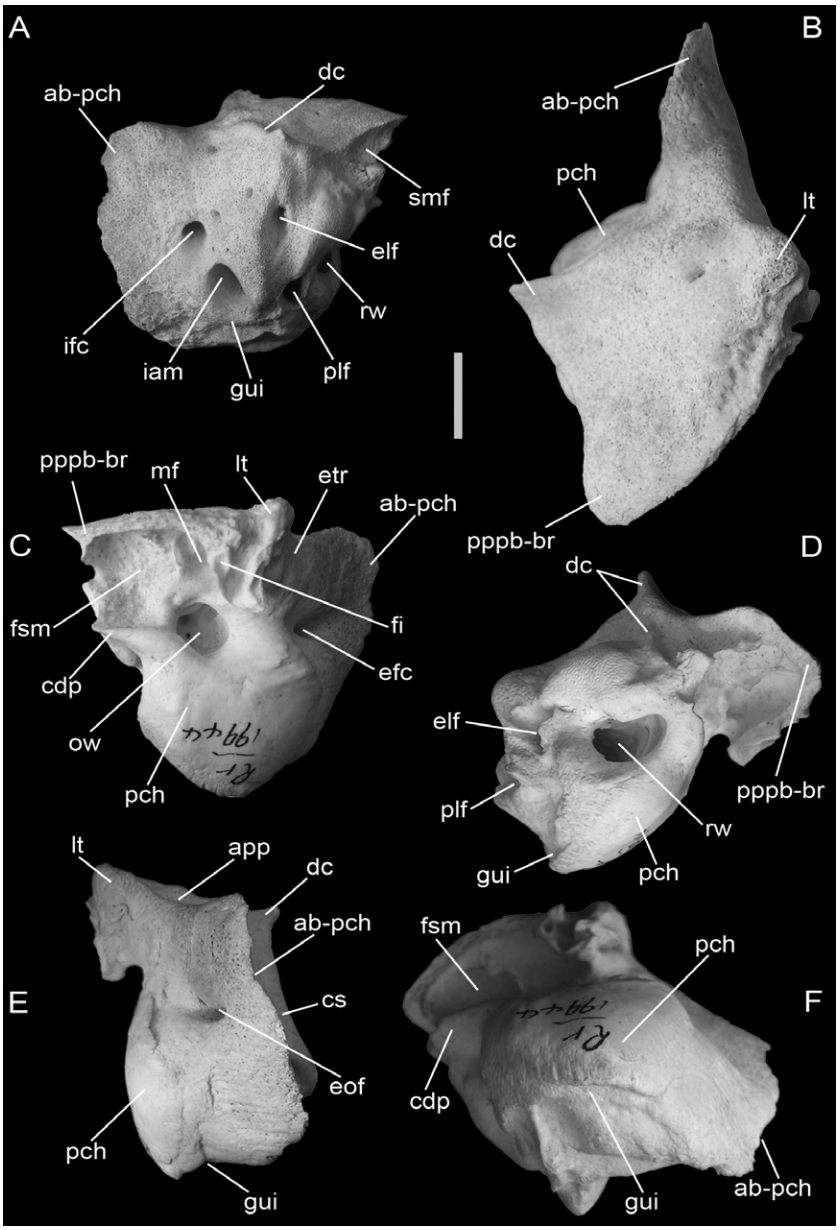

Figure 14. *Caperea marginata*: right periotic (specimen ZM 19944), detached from skull. A, medial view; B, dorsal view; C, lateral view; D, posterior view; E, anterior view; F, ventral view. Scale bar: 10 mm. See Anatomical abbreviations for definitions of the acronyms.

Dentary

Missing. Description of the dentary of *C. marginata* is provided in the Supporting information (see also Discussion, Figs 21, S5 and Table S1).

Postcranial skeleton

All the postcranial bones are missing from the holotype of *M. pulchra* gen. et sp. nov. Observations on the postcranial skeleton of *C. marginata* are published online in the Supporting information (see also Figs S6–S8 and Table S2).

PHYLOGENETIC ANALYSIS

Introduction

As noted by Beddard (1901), from a morphological point of view, Neobalaenidae are a peculiar mix of balaenopterid-like and balaenid-like characters. The presence of ventral throat grooves, dorsal fin, and

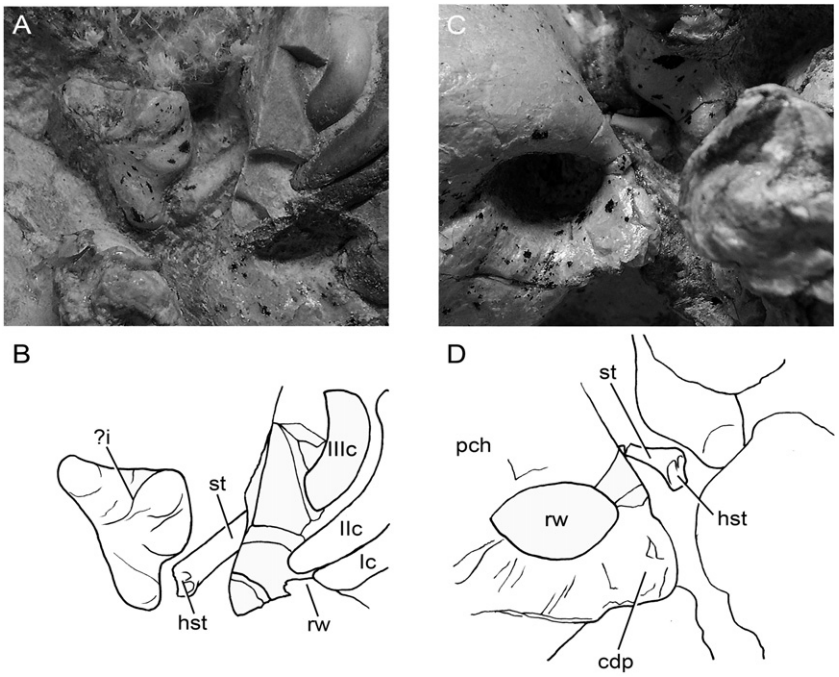

Figure 15. ***Miocaperea pulchra*** **gen. et sp. nov.**: auditory ossicles. A, right incus and stapes, *in situ*; B, schematic representation of right incus and stapes, *in situ*; C, left stapes, *in situ*; D, schematic representation of right stapes, *in situ*. See Anatomical abbreviations for definitions of the acronyms.

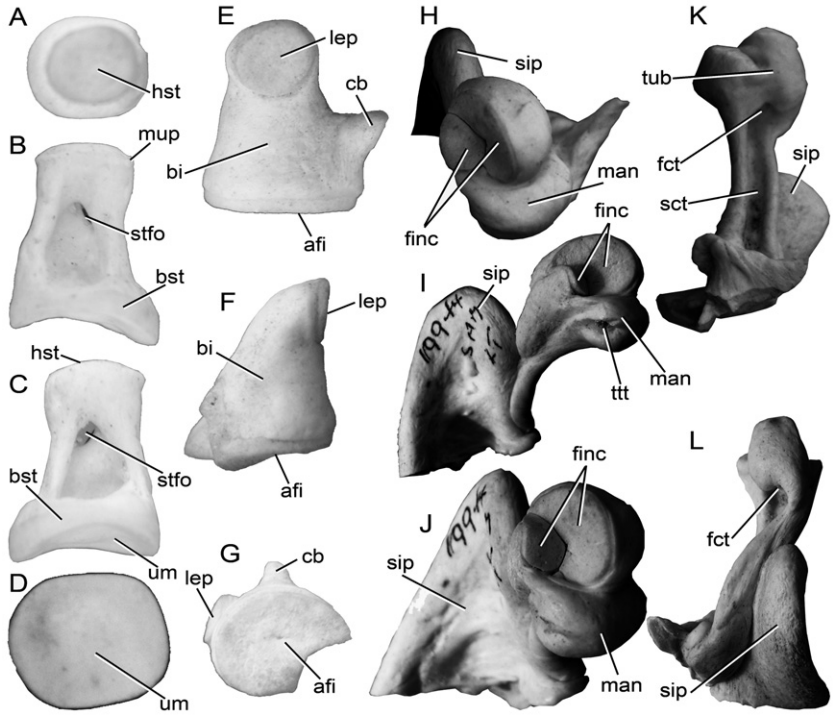

Figure 16. *Caperea marginata*: auditory ossicles – malleus, incus, and stapes. A–D, stapes; E–G, incus; H–L, malleus. Not to scale. See Anatomical abbreviations for definitions of the acronyms.

long forelimb suggest balaenopterid affinities, but their arched rostrum, comparatively long baleen, low tympanic bulla, mylohyoidal groove in the dentary, dorsally exposed mandibular condyle, absence of coronoid process, and fused cervical vertebrae support the view that they are closely related to Balaenidae (Beddard, 1901; Miller, 1923; Kellogg, 1928; McLeod, Whitmore & Barnes, 1993; Bisconti, 2003, 2005). Most molecular analyses imply, on the contrary, that the balaenid-like features result from convergent evolution (e.g. Árnason & Gullberg, 1994). The only morphology-based study that supported a sister group relationship between pygmy right and balaenopterid whales was that published by Marx (2010), and the only molecule-based work that proposed a close affinity of neobalaenids and balaenids was that of Gatesy (1998).

Some anatomical papers have emphasized the autapomorphic conditions exhibited by *C. marginata* in basicranial morphology (Fraser & Purves, 1960), vertebral column (Buchholtz, 2011), skull structure (Miller, 1923), and ribs (Beddard, 1901). Fraser & Purves (1960), in particular, suggested that the peculiar arrangement of the bones surrounding the foramen pseudo-ovale observed in *C. marginata* was an archaic condition that had subsequently disappeared in the other living mysticete families.

The fossil record was of no help in this debate because no fossil neobalaenids were known until now (Fordyce & De Muizon, 2001). The discovery of *M. pulchra* gen. et sp. nov. offers an invaluable opportunity to study evolutionary transformations in Neobalaenidae and to detect unprecedented clues of neobalaenid phylogenetic affinities. In this section, a new and comprehensive phylogenetic analysis of mysticetes is carried out, and the results are compared and discussed in a broad context that includes morphological transformations, rates of morphological evolution, and the palaeoecology and palaeobiogeography of pygmy right whales.

Material

The phylogenetic analysis was carried out through comparisons of the osteology of 46 taxa, including four archaeocetes, and two tooth-bearing and 40 baleen-bearing mysticetes. The specimens examined are presented in the Supporting information, together with their stratigraphic age and the literature relevant to their descriptions. As a whole, these taxa are representatives of all major mysticete lineages.

Methods

The phylogenetic analysis was carried out using 246 morphological characters scored for the 46 taxa listed in the Supporting information; 244 characters are from osteology and two are from baleen morphology. Character states were selected on the basis of personal observations and previous studies (McLeod *et al*., 1993; Geisler & Luo, 1996, 1998; Bisconti, 2000, 2005, 2007a, b, 2008; Kimura & Ozawa, 2002; Sanders & Barnes, 2002a; Geisler & Sanders, 2003; Deméré *et al*., 2005, 2008; Steeman, 2007, 2009; Kimura & Hasegawa, 2010). The character list and matrix are presented in the Supporting information. *Protocetus atavus* Fraas, 1904, *Georgiacetus vogtlensis* Hulbert *et al*., 1998, *Dorudon atrox* Andrews, 1906, and *Zygorhiza kochii* (Reichenbach, 1847) were selected as out-group taxa. As a whole, this is one of most inclusive analyses of mysticete phylogeny ever performed.

The data matrix was analysed by PAUP 4.0b10 (Swofford, 2002); character states were unordered and unweighted under the ACCTRAN character states optimization. The tree bisection and reconnection (TBR) algorithm with one tree held at each step during stepwise addition was used to find the most parsimonious cladograms. Character support at nodes was assessed by the apposite functions of PAUP, and synapomorphies of selected clades are provided in the Results section. The statistical support at nodes was assessed by a bootstrap analysis with 1000 replicates. A randomization test was performed to evaluate the distance of the cladograms resulting from the TBR search and 10 000 cladograms sampled equiprobably from all of the possible cladograms that can be generated using the same matrix.

To evaluate the degree of agreement of the branching order of the cladograms resulting from the TBR search and the stratigraphic occurrence of the taxa, Huelsenbeck's (1994) stratigraphic consistency index (SCI) was calculated (for a discussion of the SCI, see Bisconti, 2007a, b, 2008). Stratigraphic data were obtained mainly from the Paleobiology Database compiled by Mark D. Uhen (available at http://paleodb.org/cgi-bin/bridge.pl).

Results

Maximum parsimony

The TBR search resulted in 108 equally parsimonious trees, the strict consensus of which is shown in Figure 17 (tree statistics are presented in the corresponding caption). *Miocaperea pulchra* gen. et sp. nov. is the sister group of *C. marginata*, and both species form the monophyletic Neobalaenidae family. Neobalaenidae and Balaenidae are sister groups; their monophyly supports the inclusion of both families within the superfamily Balaenoidea. Ten characters unambiguously support the monophyly of Balaenoidea (see Supporting information), and these include: rostrum

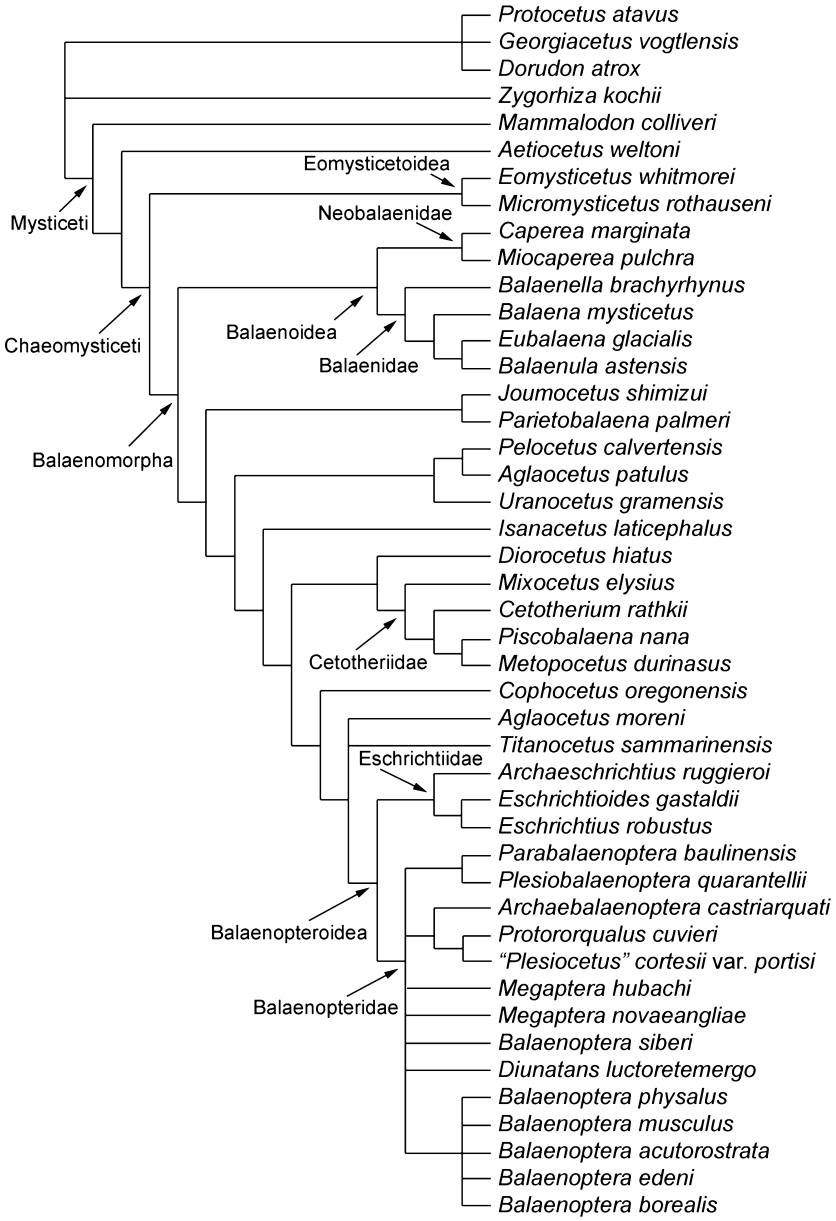

Figure 17. Phylogenetic relationships of ***Miocaperea pulchra* gen. et sp. nov.** Maximum parsimony cladogram, representing the strict consensus of 108 equally parsimonious trees. Statistics: tree length, 914 steps; consistency index, 0.3840; consistency index excluding uninformative characters, 0.3751; rescaled consistency index, 0.2732; homoplasy index, 0.6160; homoplasy index excluding uninformative characters, 0.6249; retention index, 0.7114.

highly arched (character 6, state 1); long baleen (character 14, state 0); squamosal dorsoventrally elongated (character 86, state 1); massive elongation of supraoccipital (character 104, state 1); presence of the ventral lamina of the pterygoid (character 118, state1); low dorsoventral height of tympanic cavity (character 164, state 1); epitympanic hiatus wide because of massive reduction of conical process (character 170, state 1); cervical vertebrae fused (character 200, state 1); and neural processes of cervical vertebrae 1–7 fused (character 216, state 1). Ambiguous synapomorphies include: arched rostrum (character 5, state 1; the character consistency index (CCI) is 0.5 because the state is shared with eschrichtiid whales); rostrum continuously arched (character 7, state 0; CCI is 0.667 because the character is shared with eschrichtiids, *Balaena*, and *Balaenella*); posterior lacerate foramen located very close to the posterior border of the skull (character 123, state 1; CCI is 0.5); and dorsoventral arc of the dentary continuous along the dentary (character 197,

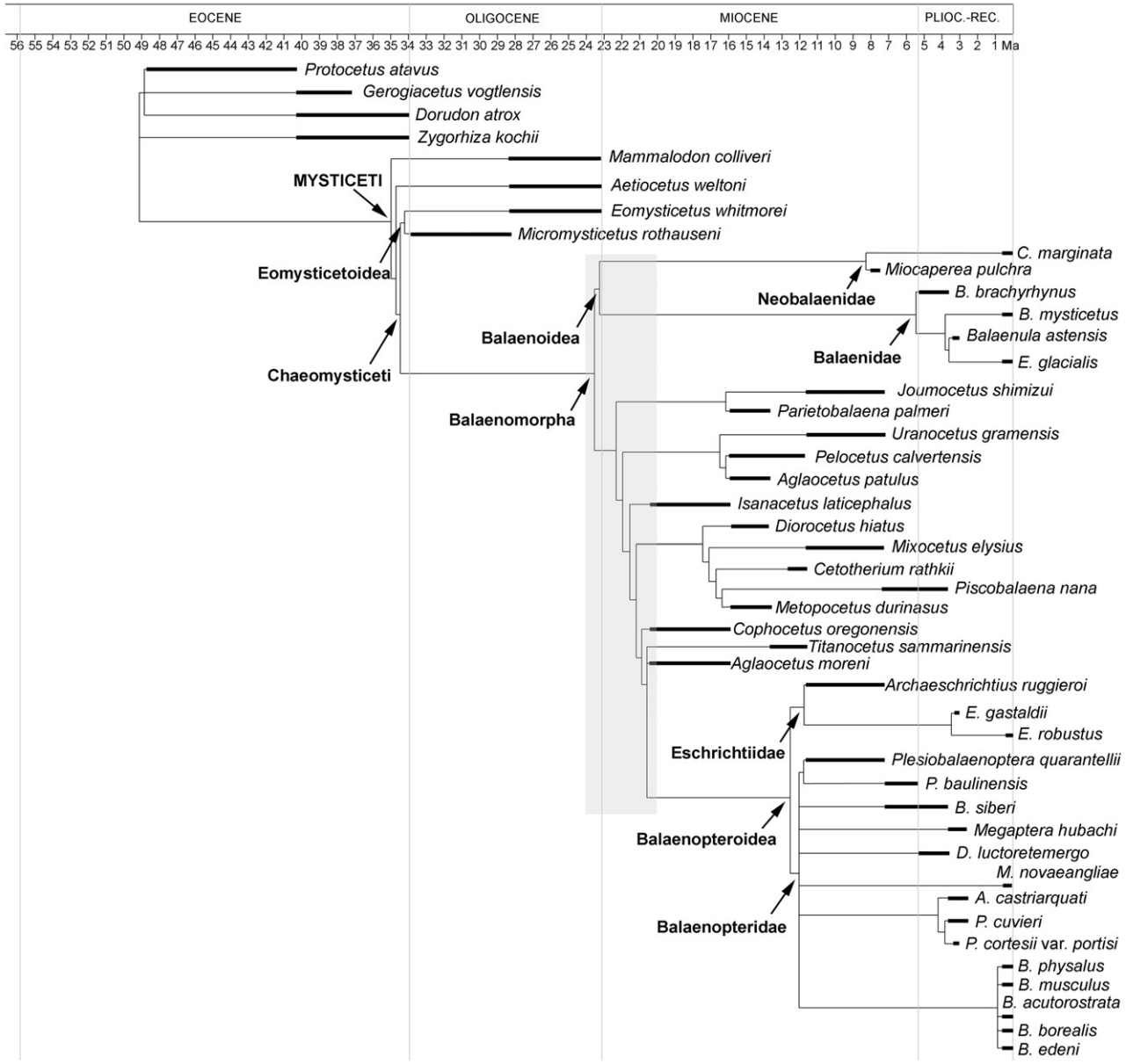

Figure 18. Phylogenetic relationships of baleen-bearing mysticetes resulting from the tree bisection and reconnection search and plotted against stratigraphic ages of the included taxa. Thick lines represent documented records; thin lines represent inferred ghost lineages. Ma, million years. The grey area represents a period of high origination rate in mysticete evolution. The divergence of Balaenidae and Neobalaenidae is calibrated on the stratigraphic age of *Morenocetus parvus*, the earliest described balaenid (the assignment to Balaenidae was confirmed by Bisconti, 2005).

state 2; CCI is 0.5 because the character is shared with eschrichtiids).

The divergence of Balaenoidea is rather old (Fig. 18) based on the stratigraphic age of the oldest known representatives of this group (*Morenocetus parvus* Cabrera, 1926 from the Aquitanian of Argentina; an Oligocene balaenid from New Zealand has been briefly presented but never formally described by Fordyce, 2002).

Balaenoidea is the sister group of an inclusive clade formed by Balaenopteridae, Eschrichtiidae, Cetotheriidae (*sensu* Bouetel & De Muizon, 2006), and a number of archaic mysticetes (*sensu* Geisler & Luo, 1996) informally called 'cetotheres'. The relation-

ships of the 'cetotheres' and of the balaenopterids are the focus of different papers (Bouetel & De Muizon, 2006; Steeman, 2009; Marx, 2010; Bisconti, 2011; M. Bisconti, O. Lambert & M. Bosselaers, unpubl. data), and are not discussed here.

Balaenopteridae and Eschrichtiidae are sister groups, and form the superfamily Balaenopteroidea (*sensu* Deméré *et al*., 2005). *Titanocetus sammarinensis* (Capellini, 1901) and *Aglaocetus moreni* Lydekker, 1894 are the sister groups of Balaenopteroidea, and their sister group is *Cophocetus oregonensis* Packard & Kellogg, 1934. There is no relationship between Balaenopteroidea and Neobalaenidae.

From the present study, convergent features of Neobalaenidae and Balaenopteridae include an anteroposteriorly elongated scapula, radius, and ulna much longer than the humerus, presence of a squamosal cleft, internal acoustic meatus separated from the endocranial opening of the facial canal, and lateral surface of the maxilla flat and not vertical.

Randomization test

The mean length of 10 000 cladograms sampled equiprobably from the set of all possible cladograms that can be found by PAUP TBR search, based on the same matrix as that provided in the Supporting information, is 2003.8398 ± 54.003 steps. As the length of the most-parsimonious TBR tree presented in Figure 17 is 914 steps, we conclude that the solution presented in this article is significantly different from chance ($P < 0.00001$).

Stratigraphic consistency index

The SCI of the cladogram presented in Figures 17 and 18 is 0.577. Such a value is rather low compared with the values reported by Bisconti (2007a, b, 2008, 2010a), which ranged from 0.7 to 0.8. The low value arises from the lack of resolution of Balaenopteridae and from the stratigraphically inconsistent position of *Aglaocetus moreni*, *Cophocetus oregonensis*, and *Isanacetus laticephalus* Kimura & Ozawa, 2002 that make several divergence dates older than expected. In the graphic representation of the stratigraphic occurrences of the taxa, the lack of agreement between the chronological assessments of the above taxa and the branching order is evident (Fig. 18).

Bootstrap

Only a few of the clades found in the maximum parsimonious trees are present in the 50% majority rule strict consensus bootstrap tree presented in Figure 19 (tree statistics are provided in the corresponding caption). In the bootstrap tree, the monophyletic Balaenopteridae (bootstrap support value is 85%) collapses into a largely unresolved node; the sister-group relationship of Balaenopteridae and Eschrichtiidae and the monophyly of Cetotheriidae still hold (bootstrap support values are, respectively, 73% and 58%). 'Cetotheres', Cetotheriidae, and Balaenopteroidea form a large and monophyletic clade supported by a high bootstrap value (86%).

The monophyly of Balaenoidea is confirmed in the bootstrap analysis by a high support value (100%), and also the monophyly of Neobalaenidae (98%) and Balaenidae (100%) are confirmed. High values are found in support of Mysticeti (89%), Chaeomysticeti (99%), and Balaenomorpha (100%), suggesting that all of these clades are valid.

DISCUSSION

Phylogenetic relationships of Neobalaenidae

The phylogenetic relationships of Neobalaenidae have been the focus of long debate. Since the early years of the 20th century, Neobalaenidae has been regarded as a complex mixture of balaenopterid and balaenid characters (Beddard, 1901; Miller, 1923; Kellogg, 1928). This observation made it difficult to resolve its phylogenetic relationships without ambiguity, even in recent years. In fact, although some morphologists found that Neobalaenidae is closely related to Balaenidae and, together with right and bowhead whales, form the superfamily Balaenoidea (McLeod *et al*., 1993; Bisconti, 2001, 2003, 2005, 2008, this work; Deméré *et al*., 2005; Steeman, 2007), molecular studies and some recent morphological analyses resulted in a close relationship of Neobalaenidae and Balaenopteroidea (*sensu* Deméré *et al*., 2005, and thus including Eschrichtiidae and Balaenopteridae) dismissing Balaenoidea as an invalid taxon (Árnason & Gullberg, 1994; Deméré *et al*., 2008; Steeman *et al*., 2009; Marx, 2010; see Gatesy, 1994 for an alternative to the standard molecular view of this topic).

The discovery of *M. pulchra* gen. et sp. nov. adds important morphological evidence that can be implemented in cladistic analyses of the mysticetes. The results of the analysis presented here confirm the monophyly of the clade that includes Balaenidae and Neobalaenidae, thus re-establishing the validity of Balaenoidea. A full list of synapomorphies that support the monophyly of Balaenoidea, together with a list of ambiguous synapomorphies, which include characters that originated independently in different lineages, are provided in the Supporting information. The ambiguous synapomorphies are particularly numerous, and include, for instance, the arched rostrum [also present in the living gray whale, *Eschrichtius robustus* (Lilljeborg, 1861)] and the presence of a mylohyoidal concavity or groove on the ventromedial side of the dentary (also present in Eschrichtiidae). Both of these characters have been

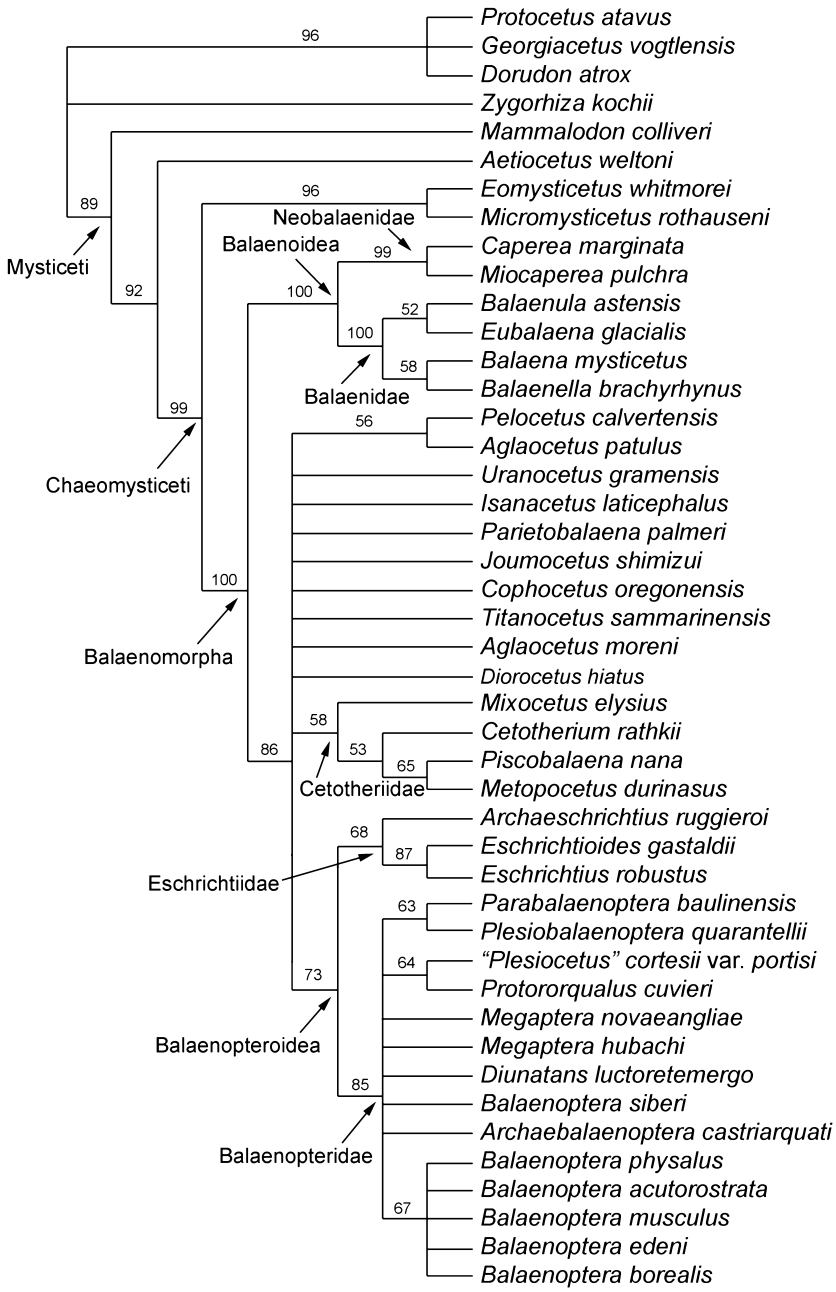

Figure 19. Phylogenetic relationships of ***Miocaperea pulchra*** **gen. et sp. nov.**: 50% majority rule strict consensus bootstrap tree. Statistics: tree length, 1068 steps; consistency index, 0.3287; consistency index excluding uninformative characters, 0.3204; rescaled consistency index, 0.2079; homoplasy index, 0.6713; homoplasy index excluding uninformative characters, 0.6796; retention index, 0.6325.

traditionally used to unambiguously support the monophyly of Balaenoidea, but according to Marx (2010) they must be regarded as ambiguous in this respect because they are also present in a lineage (Eschrichtiidae) that is not closely related to Balaenidae and Neobalaenidae. The mylohyoidal groove was not observed in all the examined neobalaenid specimens, as it was replaced, in some individuals, by a shallow concavity in the medial side of the dentary (Fig. 21; Supporting information). However, a true groove for the mylohyoidal muscle was observed in two adult specimens (ISAM ZM40626 and ISAM ZM41126), whereas it was absent in all of the juvenile ones (Fig. 21).

Unambiguous synapomorphies for Balaenoidea include a peculiar morphology of the tympanic bulla

(tympanic cavity dorsoventrally low, epytympanic hiatus particularly wide because of a strong reduction of the conical process), fusion of cervical vertebrae, strong anteroposterior development of supraoccipital, and comparatively long baleen. Based on this list of synapomorphies, the balaenopterid-like features exhibited by the neobalaenid whales must be interpreted as convergent. This includes an elongate scapula, four digits in the hand, and supraorbital process of the frontal abruptly depressed from the interorbital region of the dentary. Soft-tissue anatomy was not included in this study, thus it is not clear how the scoring of ventral throat grooves and dorsal fin (both also present in Balaenopteridae but not in Eschrichtiidae) would influence the results of the present study.

One character that supports the divergence of Neobalaenidae from Balaenopteroidea is the anatomy of the skull vertex. In fact, in most living balaenopterid species the parietal is subdivided by the interposition of the interparietal, and its anteriormost projection reaches a point located further anteriorly than the posteromedial corners of the rostrum. In Eschrichtiidae the parietal seems subdivided by the interposition of the interparietal at the cranial vertex. This is unambiguously confirmed in the Pliocene eschrichtiid *Eschrichtioides gastaldii* (Bisconti, 2008), but the condition exhibited by the living *Eschrichtius robustus* is not completely clear, even if it resembles what is seen in *E. gastaldii* very closely (for schematic representations and interpretations, see Bisconti, 2003). In Neobalaenidae the interparietal is not present and the parietal shows exactly the same pattern as that seen in Balaenidae, i.e. a strong longitudinal reduction and lack of sagittal crest (for a representation of the balaenid condition, see Bisconti, 2002).

The reconstruction of the baleen plate number of *M. pulchra* gen. et sp. nov. suggests that this whale had a maximum of around 160 baleen plates (the actual count is 156, but some baleen laminae are missing), whereas the living *C. marginata* has approximately 213–230 baleen plates (Baker, 1985; M. Bisconti, pers. observ.). In living balaenids, the number of baleen plates ranges from 205 to 346 (Cummings, 1985a; Reeves & Leatherwood, 1985). In the living *Eschrichtius robustus* there are around 180 baleen plates (Wolman, 1985) and in balaenopterids they range from around 205 to more than 400 (Cummings, 1985b; Stewart & Leatherwood, 1985). The low baleen number observed in both *Caperea* and *Miocaperea* additionally supports a close relationship with balaenid whales, as the number of baleen plates appears to be related to specialized feeding behaviour: continuous ram feeding in Balaenoidea and intermittent ram feeding in Balaenopteridae. The condition expressed by *E. robustus* (a limited baleen count) represents an independent support to this view, as *E. robustus* exhibits a mechanism of intermittent suction feeding that strongly differs from the balaenopterid feeding behaviour (Sanderson & Wassersug, 1993).

Obvious differences occurring between *M. pulchra* gen. et sp. nov. and *C. marginata* include the lack of alisphenoid exposure in the temporal fossa, a lesser posterior development of the exoccipital in *M. pulchra* gen. et sp. nov., and a different location of the foramen pseudo-ovale. The alisphenoid is exposed in the temporal fossa in a high number of baleen-bearing mysticete skulls; it is also exposed in advanced archaeocetes such as *Zygorhiza kochii* (Kellogg, 1936). The distribution of this character suggests that the alisphenoid exposure in the temporal fossa is a primitive feature in mysticetes. The lack of such an exposure in *M. pulchra* gen. et sp. nov. represents an advanced feature of this taxon.

In dorsal view, the most evident characters supporting the assignment of *M. pulchra* gen. et sp. nov. to a genus different from *Caperea* are: a reduced posterior protrusion of the posterolateral corners of the exoccipitals, a reduced posterior projection of the lambdoid crest, and a squamosal fossa nearly vertical. In *M. pulchra* gen. et sp. nov. the exoccipitals project less posteriorly and the posterior apex of the lambdoid crest is located more anteriorly. These features show that the geometry and extension of the posterior portion of the temporal fossa and of the attachment sites for the neck muscles are remarkably different in the Miocene and recent forms. Moreover, the scarce posterior development of the lambdoid crest and the nearly vertical orientation of the squamosal fossa suggest that the temporal muscle had a different morphology; this probably resulted in substantial differences in the mechanism of action of the temporal muscle during feeding. It is likely that the strong posterior protrusion of the exoccipital observed in *C. marginata* is an advanced feature typical of this form.

Fraser & Purves (1960) observed that the foramen pseudo-ovale is located within the pterygoid in *C. marginata*. In *M. pulchra* gen. et sp. nov. the foramen is located within the squamosal, as in many other baleen-bearing whales. The condition of *M. pulchra* gen. et sp. nov. is to be considered primitive given the wide distribution of this character in Balaenomorpha, and the condition of *C. marginata* is to be interpreted as an advanced feature of this taxon.

Recent investigations into the phylogeny of Cetacea in general, and on mysticetes in particular, have reinforced the hypotheses of a close relationship between Neobalaenidae, Cetotheriidae, and Balaenopteroidea (Marx, 2010; Geisler *et al.*, 2011). These studies made attempts to reconcile molecular-

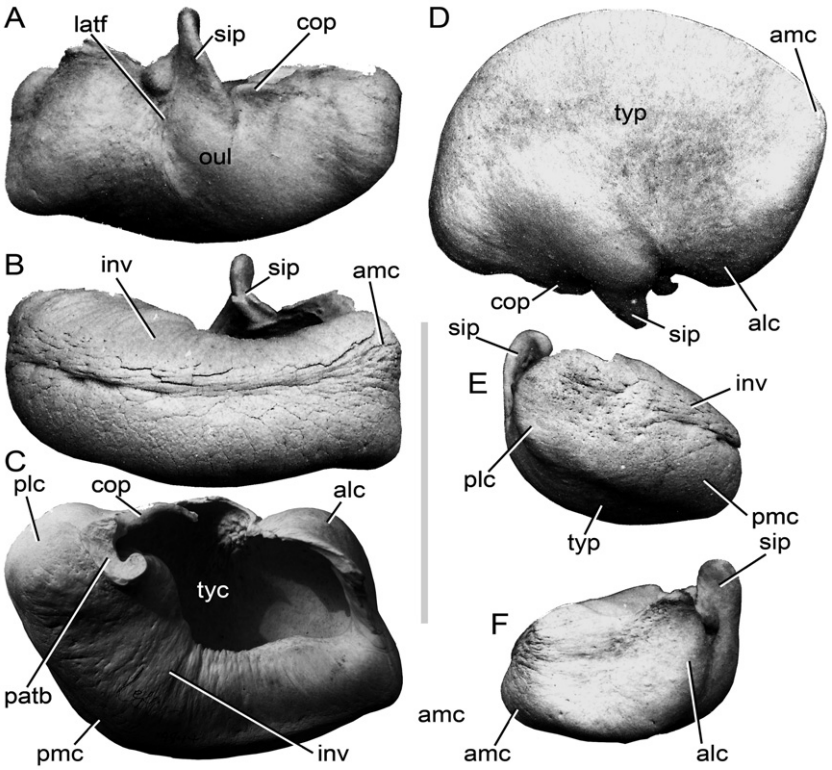

Figure 20. *Caperea marginata*: tympanic bulla. A, lateral view; B, medial view; C, dorsal view; D, ventral view; E, posterior view; F, anterior view. Scale bar: 100 mm. C, specimen ZM 19944; A, B, D–F, specimen in Klaas Post's private collection. See Anatomical abbreviations for definitions of the acronyms.

based analyses and morphology with the neobalaenid relationships. Marx (2010) provided thorough descriptions and interpretations of previously published characters in order to provide a novel view on neobalaenid phylogeny. By means of the results of his cladistic work, he was able to consider a number of character states to be plesiomorphies rather than apomorphies of a Balaenidae–Neobalaenidae clade. However, some of his interpretations are in critical need of reassessment in the light of a broader understanding of morphological variation. For instance, Marx (2010) wrote that only three character states, among those previously used by different authors, can be considered valid in support of a close relationship of Balaenidae and Neobalaenidae: (1) the anterior extension of the supraoccipital shield; (2) the fusion of the cervical vertebrae; and (3) a W-shaped anterior margin of the palatine. These characters may represent evidence in support of a close relationship of Neobalaenidae and Balaenidae, but also other characters can be used to reinforce such a hypothesis of relationship.

In particular, Marx (2010) appears to underestimate the impact of the morphology of the tympanic bulla and of the peculiar arrangement of the cranial-rostral interface of neobalaenids and balaenids. The tympanic bulla of *C. marginata* shares most of its morphology with Balaenidae (Fig. 20). In particular, the conical process is strongly reduced and shows a flat profile in lateral view (see also Ekdale, Berta & Deméré, 2011); the tympanic cavity is very low; the bulla displays a strong dorsoventral compression like that observed in other living and fossil balaenids. Marx (2010) did not include the shape of the conical process and the height of the tympanic cavity in his analysis, but these characters are among those from the present study that are crucial to support the close relationship of Neobalaenidae and Balaenidae. Marx (2010) rightly pointed out that the homology of the unusual morphology of the squamosal of Neobalaenidae could result from a peculiar evolutionary path in this family, rather than simply being homologous with that of Balaenidae. In fact, the position of the zygomatic process of the squamosal in the Neobalaenidae is more dorsal than in most balaenids. However, the ventral position of the postglenoid process of the squamosal of *Caperea* and *Miocaperea* highly resembles that observed in *Balaenula astensis* Trevisan, 1942 (Bisconti, 2001) and, more generally, the high distance between the ventralmost point of

the postglenoid process of the squamosal, the dorsal surface of the supraoccipital, and the strongly reduced anteroposterior length of the zygomatic process of the squamosal are extremely close in balaenids and neobalaenids. In this sense, the squamosal morphology of neobalaenids can be rightly interpreted as the result of a common process underlying the evolution of the squamosal in both Balaenidae and Neobalaenidae.

The arrangement of the bones at the interface between rostrum and neurocranium is rather peculiar in mysticetes, and differences in this region can be usefully adopted to distinguish different family-rank clades such as Balaenopteridae and Cetotheriidae *s.s.* (*sensu* Bouetel & de Muizon, 2006). In the case of Balaenidae and Neobalaenidae, Marx (2010) stated that the condition seen in *C. marginata* differs from that observed in *Eubalaena*, as in *Eubalaena* the interorbital region of the frontal is clearly evident in dorsal view, but in *C. marginata* such a region is substantially obliterated by the superimposition of the supraoccipital. In Figure 9, it is clearly shown that the level of exposure of the interorbital region of the frontal in *C. marginata* exhibits a degree of individual variation. In fact, in Figure 9A the frontal is reduced to a subtle stripe interposed between the supraoccipital and maxilla; in Figure 9B there is a higher extent of frontal exposed in dorsal view. It is likely that the degree of exposure of the interorbital region of the frontal depends on development, as the frontal is much more exposed in juvenile individuals and is very reduced in adult or old individuals. It is important to note that the arrangement of the bones contributing to form the cranial vertex is substantially the same in Balaenidae and Neobalaenidae, and such an arrangement can be easily distinguished from that observed in Cetotheriidae *s.s.* and *s.l.*, Eschrichtiidae, and Balaenopteridae. In particular: (1) in Balaenopteridae, in dorsal view, the ascending process of the maxilla projects much further posteriorly, forming a nearly rectangular structure, the anterior end of the parietal reaches a point more anterior than the posterior end of the ascending process of the maxilla, and an interparietal can be present; (2) in Eschrichtiidae, the condition is very similar but the parietal does not reach a point more anterior than the posterior end of the ascending process of the maxilla; (3) in Cetotheriidae *s.l.*, the anterior end of the supraoccipital is located much further posteriorly and the interparietal region is further elongated; and (4) in Cetotheriidae *s.l.*, the long ascending processes of the maxillae tend to obliterate the interorbital region of the frontal as they converge towards the longitudinal axis of the skull.

Additional evidence in support of the monophyly of Balaenoidea can be found in the morphology of the posterior portion of the dentary. Although Marx (2010) pointed out that the articular condyle of the dentary of *C. marginata* appears to be principally directed posteriorly, in Figure 21A and B it is clearly shown that most of the articular surface of the mandibular condyle of this species is directed dorsally, and is well bordered by a sharp anterior edge. Note it is possible that a dorsal articular surface could result from a developmental path starting from a further posteriorly oriented condition (see, for instance, Fig. 21D, E); thus, juvenile individuals may bear a posterior articular surface of the mandibular condyle. However, this condition is also expressed by balaenids (M. Bisconti, pers. observ. from specimen ZM 38950, *Eubalaena australis*, at the IZIKO museum in Cape Town).

An additional feature of the dentary supporting the close relationship of neobalaenids and balaenids is the shape of the angular process. Marx (2010) did not mention such a character, but it is to be noted that the angular process is relatively low and rounded in both Balaenidae and Neobalaenidae, and no clear pterygoid groove can be observed to subdivide (laterally, medially, and/or posteriorly) the condyle from the angular process. In balaenopterids, the angular process of the dentary is much lower and squared in lateral view, and a clear pterygoid groove is evident. In cetotheres, the angular process may show different morphologies but does not exhibit a round shape, as seen in Balaenoidea.

It is important to note that, apart from the studies of Marx (2010) and Deméré *et al*. (2008), all the other morphological analyses of mysticetes agreed upon the monophyly of Balaenoidea (e.g. Geisler *et al*., 2011, based on the morphological dataset only; Bisconti, 2005, 2008, 2010a; Deméré *et al*., 2005; Steeman, 2007). In the work of Geisler *et al*. (2011) the monophyly of Balaenoidea is dismissed because of the stronger support molecular data provide to a closer relationship of *Caperea* and Eschrichtiidae + Balaenopteridae.

Neobalaenid whales exhibit a mosaic of characters that will continue to puzzle researchers. The coexistence of balaenopterid-like and balaenid-like characters in the same family represents a big problem for those attempting to decipher the history of the morphological transformations that occurred in the mysticetes. New studies on the morphology of living and fossil neobalaenids are encouraged to settle this problem, and to find a shared view among morphologists and molecular biologists.

Evolutionary considerations

In Figure 18 the phylogenetic relationships of baleen-bearing mysticetes are plotted against time. Judging from the fossil record and this figure, crown mystice-

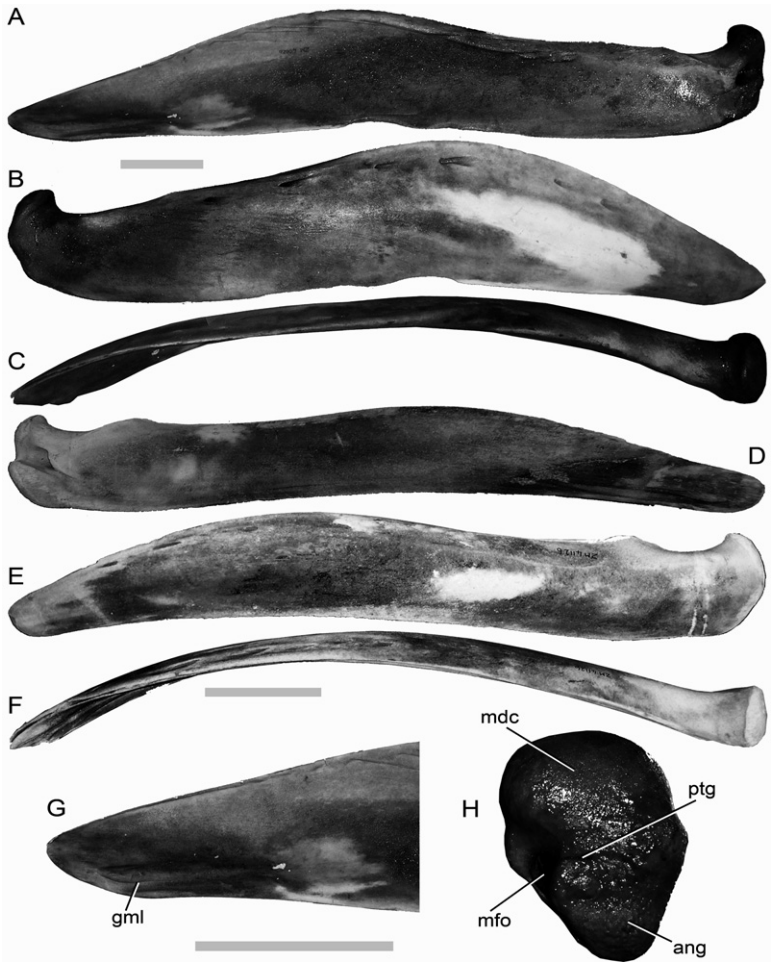

Figure 21. Individual variation of the dentary of *Caperea marginata*. ISAM ZM 40626: A, lateral view; B, medial view; C, dorsal view. ISAM ZM 41126: D, medial view; E, lateral view; F, dorsal view. G, anterior end of left dentary (ISAM ZM 40626); H, posterior end in posterior view (ISAM ZM 40626). Scale bars: 100 mm. See Anatomical abbreviations for definitions of the acronyms. ISAM ZM 41126 is a juvenile individual, characterized by an elongated and slender dentary, with dorsal border nearly parallel with the ventral border. ISAM ZM 40626 is an older individual, characterized by the higher mandibular ramus with strong raised dorsal border. Note the different orientation of the articular condyle: it is more posteriorly oriented in the juvenile (D–F), but is dorsal in the adult (A–C). Note the scarce development of the pterygoid groove separating the condyle from the angular process. The angular process is rounded and scarcely developed, resembling that of Balaenidae.

tes (Balaenomorpha) originated rather abruptly around 12 million years after the divergence of the earliest baleen whales (Eomysticetoidea). This is the time span during which the six unambiguous apomorphies of Balaenomorpha originated (see Supporting information). The grey area in Figure 18 indicates the period of major origination in Balaenomorpha; this period occurred between ~24 and ~20 Mya. In fact, in this time interval, both Balaenoidea (Balaenidae and Neobalaenidae) and the clade including Cetotheridae *s.s.* and *s.l.*, Balaenopteridae, and Eschrichtiidae originated. The presence of an early balaenid in the Late Oligocene of New Zealand, reported by Fordyce (2002), suggests that this time span could have been a little longer, possibly starting one or two million years before 24 Mya.

However, based on the present phylogeny, the morphological divergence between Balaenoidea and the other large clade occurred in the Late Oligocene; in fact, in the early Miocene the divergence was clearly established. This divergence implied the origination and establishment of two different suites of morphological characters in the two lineages (see Supporting information).

The phylogram presented in Figure 22 shows that a high number of synapomorphies is necessary to

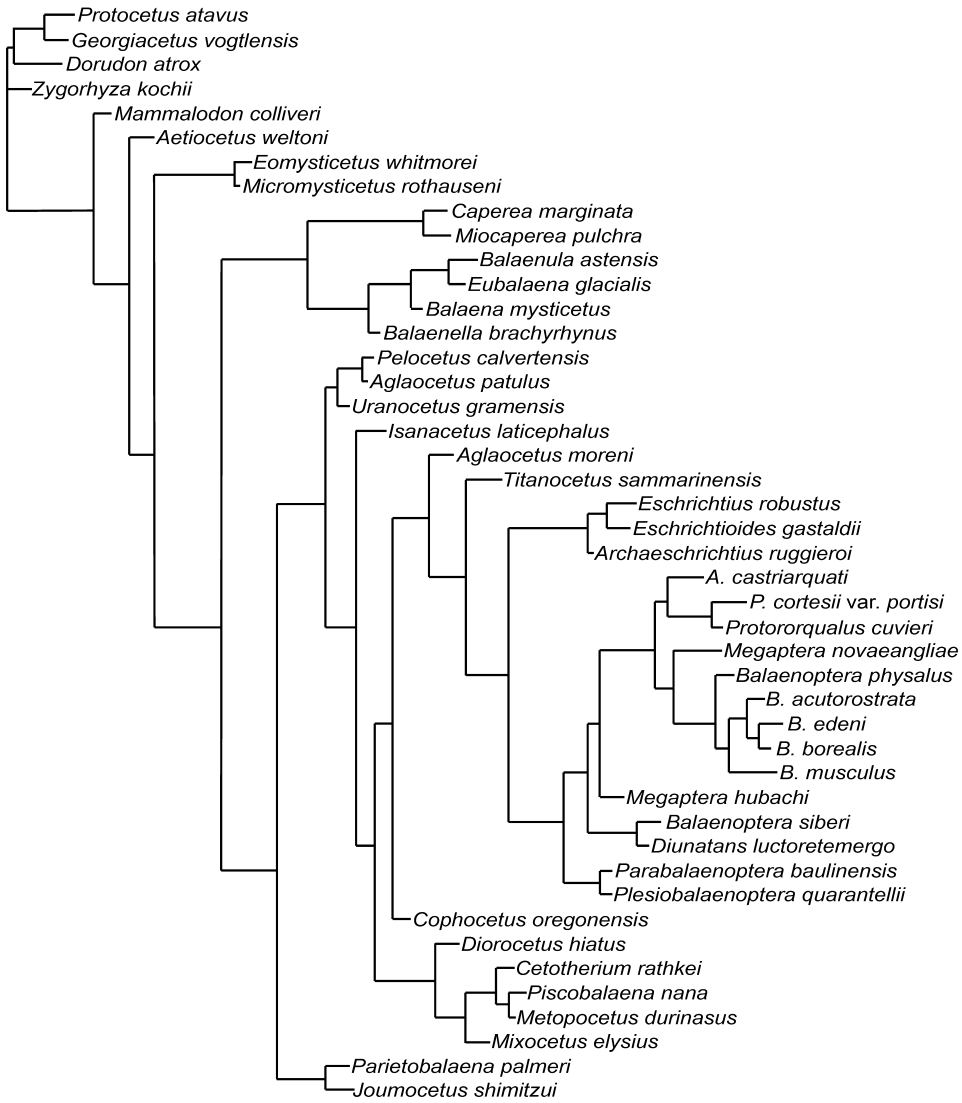

Figure 22. Phylogram showing the phylogenetic relationships of mysticetes. Branch lengths are proportional to the number of synapomorphies. Tree statistics are the same as reported in the legend to Figure 17.

interpret the origin of Balaenoidea. This observation can be explained in two ways: (1) Balaenoidea could have originated abruptly, and a strong selective regime fixed its diagnostic characters over a short time span after that; or (2) we assume that Balaenoidea had a long evolutionary history that is still unknown. In conclusion, what we need to know is the timing of the origin of Balaenoidea. We will discuss this problem below. High numbers of synapomorphies are also diagnostic of the Balaenopteroidea clade (*sensu* Deméré *et al*., 2005), including Eschrichtiidae and Balaenopteridae, a clade with a long evolutionary history that is still not completely understood (Fig. 22).

Recent studies have attempted to address whether the origin of the diversity of modern Cetacea could be described by an adaptive radiation model, by a model based on the diversity of diatoms, or by a model based on hypotheses of ocean restructuring (Steeman *et al*., 2009; Marx & Uhen, 2010; Slater *et al*., 2010). Sophisticated statistical analyses suggested that the adaptive radiation model cannot be supported by time-calibrated molecular phylogenies of living species (Steeman *et al*., 2009; Slater *et al*., 2010), but statistically significant results supported the hypotheses that the origin of cetacean diversity was linked: (1) to tectonically driven changes in the geography of the oceans influencing current patterns (Steeman *et al*., 2009) and (2) to the increase in diatom diversity (Marx & Uhen, 2010). In particular, Steeman *et al*. (2009) have suggested that the geodynamical events leading to the opening of the Drake Passage, the

restriction of the Indo-Pacific seaway, the closure of the Mediterranean–Indian ocean passage, and the closure of the Panamanian Seaway contributed to restructuring the oceanic ecosystems, resulting in high speciation rates among cetaceans. Unfortunately, they were unable to check the speciation rate in the period 28–20 Mya because they did not include fossil species in their phylogenetic reconstruction. Although their phylogenetic results are in better agreement with those of most morphologists about the position of Neobalaenidae, the lack of fossil species within their phylogeny limits the analytical power of their results. However, this is not only a problem for Steeman *et al*. (2009). In fact, Slater *et al*. (2010) also generated a phylogeny based only on living species to test their hypotheses. Despite their sophisticated analyses, the absence of the fossil record within the phylogeny is a limit that prevents them testing the hypothesis of a high speciation rate during the interval 28–20 Mya. Marx & Uhen (2010) performed a different study, principally based on the fossil record. Their work suggests that there is a link between mysticete and diatom diversity, as suggested by Kimura (2009) regarding balaenid diversity in the Pliocene.

The hypothesis presented in this paper proposes that the period 28–20 Mya was characterized by a high origination rate within the mysticetes, and is based on the hypothesis of relationships presented in Figures 17 and 18. It is to be noted that fossil mysticetes dated to such a period are relatively scarce, and include the balaenid *Morenocetus parvus* and the cetotheriid *s.l. Isanacetus laticephalus*, *Cophocetus oregonensis*, and *Aglaocetus moreni*. However, given the topology of the cladogram, it is implied that several additional lineages originated in this period. This hypothesis reinforces the model of Marx & Uhen (2010) in suggesting that the diversity of mysticetes in this period was in better agreement with the concomitant diversity of odontocetes; in turn, this would imply a lack of data about diatom diversity or a weakening of the link between cetacean and diatom diversity in the period in question.

According to Zachos *et al*. (2001), in the last 65 Myr, the $\delta^{13}C$, which represents a measure of ocean productivity, increased ~54, ~34, ~24, and ~16 Mya. The first increase was approximately coincident with the Late Palaeocene Thermal Maximum, and corresponded with (or perhaps triggered) a strong pulse of extinction among benthic faunas. The second increase corresponded to the Oi-1 glaciation that marked the beginning of the Oligocene. Steeman *et al*. (2009) suggested that the ecological conditions experienced by the oceans during this phase played a crucial role in the diversification of mysticetes. Slater *et al*. (2010) confirmed the importance of this period in their analysis of speciation rate among the whole Cetacea. These studies suggest that the assembly of the morphological characters common to all mysticetes was completed at this time (Bisconti, 2010a).

The $\delta^{13}C$ increase that occurred ~24 Mya is coincident with the Mi-1 glaciation that was followed by a series of small glaciations (Zachos *et al*., 2001). This episode corresponded to an acceleration of the Tibetan Plateau uplift and to the Andean uplift. The strong erosive regime that followed these uplift events enriched the oceans with nutrients able to sustain planktonic populations. The role played by this episode of increased productivity in the oceans on the evolution of mysticete diversity should be tested with appropriate statistical methods, but such an analysis is outside the scope of the present article. In conclusion, the present study results in a working hypothesis that suggests a link between the increase in productivity in the world oceans and a peak in mysticete diversity in the period 28–20 Mya, resulting in the establishment of all of the major mysticete lineages.

Palaeobiogeographic considerations

Currently, *C. marginata* occurs between 32°S and 52°S in latitude, irrespective of longitude (Baker, 1985; Kemper, 2002). The latitude of the type locality of *M. pulchra* gen. et sp. nov. is ~15°S, which is ~2000 km north of the northernmost sightings of *C. marginata* (Kemper, 2002). The feeding areas of *C. marginata* are not known for sure (Kemper, 2002), but analyses of stomach contents of stranded individuals revealed that the principal food items exploited by this whale are calanoid copepods (Baker, 1985; Kemper, 2002). These crustaceans feed mainly (but not exclusively) on diatoms (Klepper, 1991), and their demography is strongly linked to the availability of the nutrients that allow diatoms to form large populations, a situation that mainly occurs in the Arctic and Antarctic waters, and in upwelling zones (Razouls, Razouls & de Bovée, 2000; Hays, Richardson & Robinson, 2005).

Geological and taphonomical studies of mysticete-bearing sites in the Pisco Formation, Peru, showed that, in the Late Miocene and Early Pliocene, diatoms accumulated at extremely high rates and quickly buried the whale carcasses (Brand *et al*., 2004). This find explains the abundance of well-preserved mysticete skeletons in the area, and allows us to infer the presence of high concentrations of nutrients necessary for diatom growth. Moreover, the detection of *Chaetoceros* resting spores in the sediments (Brand *et al*., 2004), which indicate the final stages of a bloom, supports, in the Mio-Pliocene, the existence of wide and dense diatom

populations, at least during particular periods of the year in what is now Peru. Such diatom blooms depend on the local presence of nutrients made available by upwelling mechanisms (Brand *et al*., 2004, and literature therein).

Miocaperea pulchra gen. et sp. nov. exhibits skull characters consistent with those shown by continuous ram feeders, such as the living Balenoidea. These characters consist of long baleen plates, arched rostrum, and no interdigitation between rostral and neurocranial bones (Sanderson & Wassersug, 1993); therefore, its feeding mechanics were not very different from that exhibited by the living balaenoid species. For this reason, it can be inferred that *M. pulchra* gen. et sp. nov. was a continuous ram feeder, specialized to catch small prey items unable to perform complex escape behaviour, such as calanoid copepods. Its presence in waters located ~2000 km north of the northernmost occurrence of *C. marginata* is probably linked to the existence of a coastal upwelling system in the Late Miocene that supported diatom blooms and large zooplanktonic populations, close to modern-day Peru. The importance of this upwelling system probably decreased during the latest Miocene and Pliocene because of changes in current patterns, heat transport, temperatures at the surface of the sea, and nutrient availability triggered by the closure of the Panamanian Seaway, and the final and definitive establishment of the northern ice sheet in the mid-Pliocene (Schneider & Schmittner, 2006; Zachos, Dickens & Zeebe, 2008). This weakening of the coastal upwelling probably caused the shift of the neobalaenid distribution in southern waters.

From all these observations and considerations, it is possible to confirm the hypothesis of the southern Pacific origin of the continuos ram feeding in mysticetes previously proposed by Fordyce (2002), and to constraint the period of assembly of the morphological characters related to this feeding behaviour to ~28–23 Mya. The former date broadly corresponds to the age of an Oligocene balaenid from New Zealand, still to be formally described (Fordyce, 2002), and the latter to the estimated age of the oldest known balaenid, *Morenocetus parvus* (Cabrera, 1926). The divergence of Neobalaenidae and Balaenidae from stem-balaenoid ancestors should have occurred in this time interval. From the distribution of the earliest fossil balaenoid mysticetes, it is suggested that the centre of origin of Balaenoidea encompassed the southern Pacific and the southern Atlantic oceans. New studies on the Peruvian deposits should help to shed light on the morphological transformations that were responsible for the origin of the sophisticated feeding apparatus of balaenoid mysticetes.

ACKNOWLEDGEMENTS

This research was supported by funds from the Italian Ministry for University and Scientific Research ('Palaeobiogeography of Central Mediterranean from the Miocene to the Quaternary', a project co-ordinated by D. Torre, University of Florence, 2000–2002), a Collection Study Grant from the American Museum of Natural History ('Study of individual variation of right and bowhead whales', 2005), and a Synthesys 2 grant (Synthesys Project http://www.synthesys.info/), which was financed in 2010 by the European Community Research Infrastructure Action under the FP 7 (BE-TAF project no. 305). The Natuurhistorisch Museum Rotterdam funded the study of mysticete materials at ISAM. Two anonymous reviewers and the associated editor greatly improved the quality and the clarity of the article, and their effort is warmly acknowledged. Helmar P. J. Heizmann (SMNS) provided very useful and kind assistance during my visits to Stuttgart in 2001 and 2009: he informed me about the specimen and granted access to it, and he provided the necessary information about the legal status of the specimen and details of its excavation and export. Many thanks are also due to Peter Reiderle (SMNS) for his logistical help. Many thanks are due to Graham and Margaret Avery and to Leonard Compagno (all at ISAM), for their kind help during my visit to Cape Town in 2005. Richard Monk, Eric Brothers, Eileen Westwig, Maria Dickson, and Nancy Simmons (all at AMNH) greatly helped me during my study in New York in 2005. Annelise Folie and Etienne Steurbaut (all at RBINS) granted access to the RBINS collections. Finally, I want to thank Klaas Post (NMR) and Olivier Lambert (RBINS and Muséum National d'Histoire Naturelle, Paris) for their continuous encouragement and stimulus in the realization of this research.

REFERENCES

Árnason U, Gullberg A. 1994. Relationship of baleen whales established by cytochrome *b* gene sequence comparison. *Nature* **367:** 726–728.

Baker AN. 1985. Pygmy right whale *Caperea marginata* (Gray, 1846. In: Ridgway SM, Harrison R, eds. *Handbook of marine mammals*, Vol. 3. London: Academic Press, 345–354.

Barnes L, Kimura GM, Furusawa H, Sawamura H. 1995. Classification and distribution of Oligocene Aetiocetidae (Mammalia; Cetacea; Mysticeti) from western North America and Japan. *The Island Arc* **3:** 392–431.

Beddard FE. 1901. Contribution towards a knowledge of the osteology of the pigmy whale (*Neobalaena marginata*). *Transactions of the Zoological Society* **16:** 87–108.

Bisconti M. 2000. New description, character analysis and preliminary phyletic assessment of two Balaenidae skulls from the Italian Pliocene. *Palaeontographia Italica* **87:** 37–66.

Bisconti M. 2001. Morphology and postnatal growth trajectory of rorqual petrosal. *Italian Journal of Zoology* **68:** 87–93.

Bisconti M. 2002. An early Late Pliocene right whale (genus *Eubalaena*) from Tuscany (Central Italy). *Bollettino Della Società Paleontologica Italiana* **41:** 83–91.

Bisconti M. 2003. Evolutionary history of Balaenidae. *Cranium* **20:** 9–50.

Bisconti M. 2005. Morphology and phylogenetic relationships of a new diminutive balaenid from the lower Pliocene of Belgium. *Palaeontology* **48:** 793–816.

Bisconti M. 2006. *Titanocetus*, a new baleen whale from the Middle Miocene of northern Italy (Mammalia, Cetacea, Mysticeti). *Journal of Vertebrate Paleontology* **26:** 344–354.

Bisconti M. 2007a. Taxonomic revision and phylogenetic relationships of the rorqual-like mysticete from the Pliocene of Mount Pulgnasco, northern Italy (Mammalia, Cetacea, Mysticeti). *Palaeontographia Italica* **91:** 85–108.

Bisconti M. 2007b. A new basal balaenopterid from the Early Pliocene of northern Italy. *Palaeontology* **50:** 1103–1122.

Bisconti M. 2008. Morphology and phylogenetic relationships of a new eschrichtiid genus (Cetacea: Mysticeti) from the Early Pliocene of northern Italy. *Zoological Journal of the Linnean Society* **153:** 161–186.

Bisconti M. 2010a. A new balaenopterid whale from the Late Miocene of the Stirone River, northern Italy (Mammalia, Cetacea, Mysticeti). *Journal of Vertebrate Paleontology* **30:** 943–958.

Bisconti M. 2010b. Cenozoic environmental changes and evolution of baleen whales. In: Murray CA, ed. *Whales and dolphins. Behavior, biology and distribution*. New York: Nova Science Publishers, 1–46.

Bisconti M. 2011. New description of *'Megaptera' hubachi* Dathe, 1983 based on the holotype skeleton held in the Museum für Naturkunde, Berlin. Bisconti M, Roselli A, Borzatti de Loewenstern A eds. *Climatic Change, Biodiversity, Evolution: Natural History Museum and Scientific Research. Proceedings of the Meeting. Quaderni del Museo di Storia Naturale di Livorno* 23: 37–68.

Bisconti M, Varola A. 2000. Functional hypothesis on an unusual mysticete dentary with double coronoid process from the Miocene of Apulia and its systematic and behavioural implications. *Palaeontographia Italica* **87:** 19–35.

Bisconti M, Varola A. 2006. The oldest eschrichtiid mysticete and a new morphological diagnosis of Eschrichtiidae. *Rivista Italiana Di Paleontologia E Stratigrafia* **119:** 447–457.

Bosselaers M, Post K. 2010. A new fossil rorqual (Mammalia, Cetacea, Balaenopteridae) from the Early Pliocene of the North Sea, with a review of the rorqual species described by Owen and Van Beneden. *Geodiversitas* **32:** 331–363.

Bouetel V, de Muizon C. 2006. The anatomy and relationships of *Piscobalaena nana* (Cetacea, Mysticeti), a Cetotheriidae s.s. from the early Pliocene of Peru. *Geodiversitas* **28:** 319–395.

Brand LR, Esperante R, Chadwick AV, Poma Porras O, Alomìa M. 2004. Fossil whale preservation implies high diatom accumulation rate in the Miocene-Pliocene Pisco Formation of Peru. *Geology* **32:** 165–168.

Brandt JF. 1873. Untersuchungen uber die fossilen und subfossilen Cetaceen Europas. *Memoires De l'Academie Imperiale Des Sciences, St. Pétersburg* **7:** 1–54.

Buchholtz EA. 2011. Vertebral and rib anatomy in *Caperea marginata*: Implications for evolutionary patterning of the mammalian vertebral column. *Marine Mammal Science* **27:** 382–397.

Cabrera A. 1926. Cetaceos fossiles del Museo de La Plata. *Revista Del Museo De La Plata* **29:** 363–411.

Cummings WC. 1985a. Right whales – *Eubalaena glacialis and Eubalaena australis*. In: Ridgway SM, Harrison R, eds. *Handbook of marine mammals*, Vol. 3. London: Academic Press, 275–304.

Cummings WC. 1985b. Bryde's whale – *Balaenoptera edeni* Anderson, 1878. In: Ridgway SM, Harrison R, eds. *Handbook of marine mammals*, Vol. 3. London: Academic Press, 137–170.

Dathe F. 1983. *Megaptera hubachi* n. sp., ein fossiler Bartenwal aus marinen Sandsteinschichten des tieferen Pliozäns Chiles. *Zeitscrift Für Geological Wissenschaften* **11:** 813–852.

De Muizon C. 1988. Les vertébrés fossiles de la Formation Pisco (Pérou). Troisième partie: les odontocètes (Cetacea, Mammalia) du Miocène. *Institut Francoise d'Étude Andines Memoires* **78:** 1–244.

De Muizon C, Bellon H. 1981. L'âge mio-pliocène de la Formation Pisco (Pérou). *Comptes Rendus Hebdomadaire Seances Academie Sciences Paris D* **290:** 1063–1066.

De Muizon C, DeVries TJ. 1985. Geology and paleontology of late Cenozoic marine deposits in the Sacaco Area (Peru). *Geologische Rundschau* **74:** 547–563.

De Muizon C, Mc Donald G, Salas R, Urbina M. 2003. A new early species of the aquatic sloth *Thalassocnus* (Mammalia, Xenarthra) from the Late Miocene of Peru. *Journal of Vertebrate Paleontology* **23:** 886–894.

Deméré RA, Berta A. 2009. Skull anatomy of the Oligocene toothed mysticete *Aetioceus weltoni* (Mammalia; Cetacea): implications for mysticete evolution and functional anatomy. *Zoological Journal of the Linnean Society* **154:** 308–352.

Deméré TA, Berta A, McGowen MR. 2005. The taxonomic and evolutionary history of fossil and modern balaenopteroid mysticetes. *Journal of Mammalian Evolution* **12:** 99–143.

Deméré TA, McGowen MR, Berta A, Gatesy J. 2008. Morphological and molecular evidence for a stepwise evolutionary transition from teeth to baleen in mysticete whales. *Systematic Biology* **57:** 15–37.

Ekdale EG, Berta A, Deméré TA. 2011. The comparative osteology of the petrotympanic complex (ear region) of extant baleen whales (Cetacea: Mysticeti). *PLoS ONE* **6:** e21311. (doi:10.1371/journal.pone.0021311).

Ferrero E, Pavia G. 1996. La successione marina previllanoviana. Carraro F, ed. Revisione del Villafranchiano nell'area-tipo di Villafranca d'Asti. *Il Quaternario* **9:** 36–38.

Fitzgerald EMG. 2010. The morphology and systematics of *Mammalodon colliveri* (Cetacea: Mysticeti), a toothed mysticete from the Oligocene of Australia. *Zoological Journal of the Linnean Society* **158:** 367–476.

Fitzgerald EMG. 2012. Possibile neobalaenid from the Miocene of Australia implies a long evolutionary history for the pygmy right whale *Caperea marginata* (Cetacea, Mysticeti). *Journal of Vertebrate Paleontology* **32:** 976–980.

Fleischer G. 1976. Hearing in extinct cetaceans as determined by cochlear structure. *Journal of Paleontology* **50:** 133–152.

Fordyce RE. 2002. Oligocene origins of skim-feeding right whales: a small archaic balaenid from New Zealand. *Journal of Vertebrate Paleontology* **22** (Suppl.): 54a.

Fordyce RE. 2009. Cetacean evolution. In: Perrin WF, Thewissen JGM, Würsig B, eds. *Encyclopedia of marine mammals*. San Diego, CA: Elsevier, 201–207.

Fordyce RE, de Muizon C. 2001. Evolutionary history of whales: a review. In: Mazin J-M, de Buffrenil V, eds. *Secondary adaptation of tetrapods to life in water. Proceedings of the international meeting*. München: Verlag Dr Friedriech Pfeil, 169–234.

Fraas E. 1904. Neue Zeuglodonten aus dem Unteren Mitteleocän vom Mokattam bei Cairo. *Geologisches Und Palaeontologisches Abhandlungen* **6:** 199–220.

Fraser FC, Purves PE. 1960. Hearing in cetaceans. *Bulletin of the British Museum (Natural History), Zoology* **7:** 1–140.

Gambell R. 1985a. Sei whale – *Balaenoptera borealis*. In: Ridgway SM, Harrison R, eds. *Handbook of marine mammals*, Vol. 3. London: Academic Press, 155–170.

Gambell R. 1985b. Fin whale – *Balaenoptera physalus*. In: Ridgway SM, Harrison R, eds. *Handbook of marine mammals*, Vol. 3. London: Academic Press, 171–192.

Gatesy J. 1994. Molecular evidence for the phylogenetic affinities of Cetacea. In: Thewissen JGM, ed. *The emergence of whales: evolutionary patterns in in the origin of Cetacea*. New York: Plenum Press, 63–111.

Gatesy J. 1998. Molecular evidence for the phylogenetic affinities of Cetacea. In: Thewissen JGM, ed., *The emergence of whales: evolutionary patterns in the origin of Cetacea*. New York: Plenum Press, 63–111.

Geisler JH, Luo Z. 1996. The petrosal and inner ear of *Herpetocetus* sp. (Mammalia: Cetacea) and their implications for the phylogeny and hearing of archaic mysticetes. *Journal of Paleontology* **70:** 1045–1066.

Geisler JH, Luo Z. 1998. Relationships of Cetacea to terrestrial Ungulates and the evolution of cranial vasculature in Cete. In: Thewissen JGM, ed. *The emergence of whales: evolutionary patterns in in the origin of Cetacea*. New York: Plenum Press, 163–212.

Geisler JH, McGowen MR, Yang G, Gatesy J. 2011. A supermatrix analysis of genomic, morphological, and paleontological data from crown Cetacea. *BMC Evolutionary Biology* **11:** 112–145.

Geisler JH, Sanders AE. 2003. Morphological evidence for the phylogeny of Cetacea. *Journal of Mammalian Evolution* **10:** 23–129.

Hays GC, Richardson AJ, Robinson C. 2005. Climate change and marine plankton. *Trends in Ecology and Evolution* **20:** 337–344.

Huelsenbeck JP. 1994. Comparing the stratigraphic record to estimates of phylogeny. *Paleobiology* **20:** 470–483.

Hulbert, RC Jr. 1998. Postcranial osteology of the North American Middle Eocene protocetid *Georgiacetus*. In: Thewissen JGM, ed. *The emergence of whales*. New York: Plenum Press, 235–267.

Hulbert, RC Jr, Petkewich RM, Bishop GA, Bukry D, Aleshire DP. 1996. A new Middle Eocene protocetid whale (Mammalia: Cetacea: Archaeoceti) and associated biota from Georgia. *Journal of Paleontology* **72:** 907–927.

Kellogg R. 1928. The history of whales – their adaptation to life in the water. *Quarterly Review of Biology* **3:** 29–76; and 174–208.

Kellogg R. 1934a. The Patagonia fossil whalebone whale, *Cetotherium moreni* (Lydekker). *Carnegie Museum Washington Publication* **447:** 63–81.

Kellogg R. 1934b. A new cetothere from the Modelo Formation at Los Angeles, California. *Contributions in Palaeontology, Carnegie Institution Washington* **447:** 85–104.

Kellogg R. 1936. A review of the Archaeoceti. *Carnegie Institution Washington* **482:** 1–366.

Kellogg R. 1965. A new whalebone whale from the Miocene Calvert Formation. *United States National Museum Bulletin* **247:** 1–45.

Kellogg R. 1968. Fossil marine mammals from the Miocene Calvert Formation of Maryland and Virginia. *United States National Museum Bulletin* **247:** 103–197.

Kemper CM. 2002. Distribution of the pygmy right whale, *Caperea marginata*, in the Australasian region. *Marine Mammal Science* **18:** 99–111.

Kimura T. 2009. Review of the fossil balaenids from Japan with a re-description of *Eubalaena shinshuensis* (Mammalia, Cetacea, Mysticeti). *Quad. Mus. St. Nat. Livorno* **22:** 3–21.

Kimura T, Hasegawa Y. 2010. A new baleen whale (Mysticeti: Cetotheriidae) from the earliest Late Miocene of Japan and a reconsideration of the phylogeny of cetotheres. *Journal of Vertebrate Paleontology* **30:** 577–591.

Kimura T, Ozawa T. 2002. A new cetothere (Cetacea: Mysticeti) from the Early Miocene of Japan. *Journal of Vertebrate Paleontology* **22:** 684–702.

Klepper GS, Holliday DV, Pieper RE. 1991. Trophic interactions between copepods and microplankton: A question about the role of diatoms. *Limnology and Oceanography* **36:** 172–178.

Klepper GS. 1993. On the diet of calanoid copepods. *Marine Ecology Progress Series* **99:** 183–195.

Marx FG. 2010. The More the Merrier? A Large Cladistic Analysis of Mysticetes, and Comments on the Transition from Teeth to Baleen. *Journal of Mammalian Evolution* **18:** 77–100.

Marx FG, Uhen MD. 2010. Climate, critters, and cetaceans:

Cenozoic drivers of the evolution of modern whales. *Science* **327:** 993–996.

McLeod SA, Whitmore, FC Jr, Barnes LG. 1993. Evolutionary relationships and classification. Burns JJ, Montague JJ, Cowles CJ, eds. The bowhead whale. *The Society for Marine Mammalogy, Special Publication* **2:** 45–70.

Mead JG, Fordyce RE. 2010. The therian skull. A lexicon with emphasis on the odontocetes. *Smithsonian Contributions to Zoology* **627:** 1–248.

Miller GS. 1923. The telescoping of the cetacean skull. *Smithsonian Miscellaneous Collections* **76:** 1–70.

Nickel R, Schummer A, Seiferle E. 1991. *Trattato di anatomia degli animali domestici, Vol. 1.* Bologna: Edagricole.

Nikaido M, Hamilton H, Makino H, Sasaki T, Takahashi K, Goto M, Kanda N, Pastene LA, Okada N. 2006. Baleen whale phylogeny and a past extensive radiation event revealed by SINE insertion analysis. *Molecular Biology and Evolution* **23:** 866–873.

Packard EL, Kellogg R. 1934. A new cetothere from the Miocene Astoria Formation of Newport, Oregon. *Publications of the Carnegie Institution Washington* **447:** 1–62.

Pilleri G. 1989. *Balaenoptera siberi*, ein neuer Spätmiozäner Bartenwal aus der Pisco-Formation Perus. In: Pilleri G, ed. *Beiträge zur Paläontologie der Cetaceen Perus*. Bern: Hirnanatomisches Institut Ostermundigen, 65–107.

Portis A. 1885. Catalogo descrittivo dei Talassoterii rinvenuti nei terreni terziari del Piemonte e della Liguria. *Memorie Della Reale Accademia Delle Scienze Di Torino* **37:** 247–365.

Razouls S, Razouls C, de Bovée F. 2000. Biodiversity and biogeography of Antarctic copepods. *Antarctic Sciences* **12:** 343–362.

Reeves RR, Leatherwood S. 1985. Bowhead whale – *Balaena mysticetus*. In: Ridgway SM, Harrison R, eds. *Handbook of marine mammals*, Vol. 3. London: Academic Press, 305–344.

Sanders AE, Barnes LG. 2002a. Paleontology of the Late Oligocene Ashley and Chandler Bridge Formations of South Carolina, 2: *Mycromysticetus rothauseni*, a primitive cetotheriid mysticete (Mammalia: Cetacea). Emry RJ, ed. Cenozoic mammals of land and sea: tributes to the career of Clayton E. Ray. *Smithsonian Contributions in Paleobiology* 97: 271–293.

Sanders AE, Barnes LG. 2002b. Paleontology of the late oligocene ashley and chandler bridge formations of South Carolina, 3: Eomysticetidae, a new family of primitive mysticetes (Mammalia: Cetacea). Emry RJ, ed. Cenozoic mammals of land and sea: tributes to the career of Clayton E. Ray. *Smithsonian Contribution to Paleobiology* 93: 313–356.

Sanderson LR, Wassersug R. 1993. Convergent and alternative designs for vertebrate suspension feeding. In: Hanken J, Hall BK, eds. *The skull. Volume 3: Functional and evolutionary mechanisms*. Chicago, IL: University Press of Chicago, 37–112.

Sasaki T, Nikaido M, Hamilton H, Goto M, Kato H, Kanda N, Pastene LA, Cao Y, Fordyce RE, Hasegawa M, Okada N. 2005. Mitochondrial phylogenetics and evolution of mysticete whales. *Systematic Biology* **54:** 77–99.

Schaller O. 1999. *Nomenclatura anatomica veterinaria illustrata*. Roma: Delfino Editore.

Schneider B, Schmittner A. 2006. Simulating the impact of the Panamanian seaway closure on ocean circulation, marine productivity and nutrient cycling. *Earth and Planetary Science Letters* **246:** 367–380.

Slater GJ, Price SA, Santini F, Alfaro ME. 2010. Diversity versus disparity and the radiation of modern Cetacea. *Proceedings of the Royal Society B* **277:** 3097–3104.

Steeman ME. 2007. Cladistic analysis and a revised classification of fossil and recent mysticetes. *Zoological Journal of the Linnean Society* **150:** 875–894.

Steeman ME. 2009. A new baleen whale from the Late Miocene of Denmark and early mysticete hearing. *Palaeontology* **52:** 1169–1190.

Steeman ME, Hebsgaard MB, Fordyce RE, Simon YWH, Rabosky DL, Nielsen R, Rahbek C, Glenner H, Rensen MVS, Willersle E. 2009. Radiation of extant Cetaceans driven by restructuring of the oceans. *Systematic Biology* **58:** 573–585.

Stewart BS, Leatherwood S. 1985. Minke whale – *Balaenoptera acutorostrata*. In: Ridgway SM, Harrison R, eds. *Handbook of marine mammals*, Vol. 3. London: Academic Press, 91–136.

Struthers J. 1895. On the carpus of the Greenland right whale (*Balaena mysticetus*) and of fin-whales. *Journal of Anatomy and Physiology* **29:** 145–187.

Swofford DL. 2002. PAUP – Phylogenetic Systematics Using Parsimony. Beta Documentation. Washington, DC: Laboratory of Molecular Systematics, Smithsonian Institution. Available at: http://paup.csit.fsu.edu/

Trevisan L. 1941. Una nuova specie di *Balaenula* pliocenica. *Palaeontographia Italica* **40:** 1–13.

Uhen MD. 1998. Middle to Late Eocene basilosaurines and dorudontines. In: Thewissen JGM, ed. *The emergence of whales: evolutionary patterns in in the origin of Cetacea*. New York: Plenum Press, 29–63.

Uhen MD. 2004. Form, function, and anatomy of *Dorudon atrox* (Mammalia, Cetacea): an archaeocete from the middle to late Eocene of Egypt. *University of Michigan, Papers in Paleontology* **34:** 1–222.

Winn HE, Reichley NE. 1985. Humpback whale – *Megaptera novaeangliae*. In: Ridgway SM, Harrison R, eds. *Handbook of marine mammals*, Vol. 3. London: Academic Press, 241–274.

Wolman AA. 1985. Gray whale – *Eschrichtius robustus*. In: Ridgway SM, Harrison R, eds. *Handbook of marine mammals*, Vol. 3. London: Academic Press, 67–90.

Yochem PK, Leatherwood S. 1985. Bowhead whale – *Balaena mysticetus*. In: Ridgway SM, Harrison R, eds. *Handbook of marine mammals*, Vol. 3. London: Academic Press, 305–354.

Zachos JC, Dickens GR, Zeebe RE. 2008. An early Cenozoic perspective on greenhouse warming and carbon-cycle dynamics. *Nature* **45:** 279–283.

Zachos JC, Pagani M, Sloan L, Thomas E, Billups K. 2001. Trends, rhythms, and aberrations in global climate 65 Ma to present. *Science* **292:** 686–693.

Zeigler CV, Chan GL, Barnes LG. 1997. A new Late Miocene balaenopterid whale (Cetacea: Mysticeti), *Parabalaenoptera baulinensis*, (new genus and species) from the Santa Cruz Mudstone, Point Reyes Peninsula, California. *Proceedings of the California Academy of Sciences* **50:** 115–138.

SUPPORTING INFORMATION

Additional supporting information may be found in the online version of this article:

Figure S1. Individual variation in the skull of *Caperea marginata*.
Figure S2. *Caperea marginata*: schematic representations of skull.
Figure S3. Individual variation of the skull of *Caperea marginata* in lateral view.
Figure S4. *Caperea marginata*: transverse sections of the rostrum (specimen ZM 40626).
Figure S5. Individual variation of the dentary of *Caperea marginata*.
Figure S6. Skeletons of *Caperea marginata*.
Figure S7. Postcranial skeleton of *Caperea marginata*.
Figure S8. *Caperea marginata* (specimen AMO 36692): cervical vertebrae.
Table S1. Measurements of dentary in *Caperea marginata*.
Table S2. Measurements of postcranial skeleton in *Caperea marginata*.